REPORT 964

THE EFFECTS OF VARIATIONS IN REYNOLDS NUMBER BETWEEN 3.0×10^6 AND 25.0×10^6 UPON THE AERODYNAMIC CHARACTERISTICS OF A NUMBER OF NACA 6-SERIES AIRFOIL SECTIONS

By LAURENCE K. LOFTIN, JR., and WILLIAM J. BURSNALL

SUMMARY

Results are presented of an investigation made to determine the two-dimensional lift and drag characteristics of nine NACA 6-series airfoil sections at Reynolds numbers of 15.0×10^6, 20.0×10^6, and 25.0×10^6. Also presented are data from NACA Rep. 824 for the same airfoils at Reynolds numbers of 3.0×10^6, 6.0×10^6, and 9.0×10^6. The airfoils selected represent sections having variations in the airfoil thickness, thickness form, and camber. The characteristics of an airfoil with a split flap were determined in one instance, as was the effect of surface roughness. Qualitative explanations in terms of flow behavior are advanced for the observed types of scale effect.

INTRODUCTION

Two-dimensional aerodynamic data obtained at Reynolds numbers of 3.0×10^6, 6.0×10^6, and 9.0×10^6 are now generally available for a large number of systematically derived NACA airfoil sections (reference 1). The Reynolds number range from 3.0×10^6 to 9.0×10^6 is sufficient to satisfy engineering needs for many practical applications, but the recent trends toward both very large and very high-speed aircraft have emphasized the necessity for aerodynamic data at higher values of the Reynolds number. An investigation has accordingly been made of the aerodynamic characteristics of a number of systematically varied NACA 6-series airfoils at Reynolds numbers of 15.0×10^6, 20.0×10^6, and 25.0×10^6. The results of this investigation at high Reynolds numbers together with those from reference 1 for the same airfoils at Reynolds numbers of 3.0×10^6, 6.0×10^6, and 9.0×10^6 are presented in the present report. These results are analyzed, and possible qualitative explanations in terms of flow behavior are advanced for the type of scale effects observed.

The airfoil design parameters varied were the thickness, thickness form, and camber. The NACA 63 series was chosen as the basic group for investigation because, on the basis of available information, these airfoils appear to offer good low-speed characteristics with a minimum of compromise from consideration of the high-speed characteristics. Symmetrical airfoils of this series having thickness ratios of 6, 9, 12, and 18 percent of the chord were tested. Variations in the thickness form were investigated for thickness ratios of 6 and 9 percent of the chord, and the effect of a small amount of camber was determined for thickness ratios of 9 percent and 12 percent of the chord. The systematic investigation was made with the airfoils in the smooth condition, although the effects of surface roughness were determined in one instance. One test was also made with an airfoil equipped with a trailing-edge split flap. In all cases, only lift and drag were measured.

COEFFICIENTS AND SYMBOLS

c	airfoil chord
c_d	section drag coefficient
$c_{d_{min}}$	minimum section drag coefficient
c_l	section lift coefficient
$c_{l_{max}}$	maximum section lift coefficient
R	Reynolds number based on airfoil chord and free-stream velocity
R'	Reynolds number based on distance between laminar separation point and transition point and local velocity outside the boundary layer at the point of separation
α_0	section angle of attack

APPARATUS AND TESTS

Wind tunnel.—All the tests were made in the Langley two-dimensional low-turbulence pressure tunnel. The test section of this tunnel measures 3 feet by 7.5 feet and the model, when mounted, completely spanned the 3-foot dimension. Seals in the form of felt-back, wooden end plates were installed between the ends of the model and the tunnel walls to prevent air leakage. Lift measurements were made by taking the difference between the pressure reaction upon the floor and ceiling of the tunnel. Drag results were obtained by the wake-survey method. A more complete description of the tunnel and the method of obtaining and reducing the data may be found in reference 2.

Models.—The nine airfoil sections for which experimental aerodynamic characteristics were obtained are:

NACA 63–006	NACA 64–006	NACA 65–006
NACA 63–009	NACA 64–009	
NACA 63_1–012		
NACA 63_3–018		
NACA 63–209		
NACA 63_1–212		

The models representing the airfoil sections were of 24-inch chord and, with the exception of the model of the NACA 63_3–018 airfoil which was made of laminated mahogany, all were of machined metal. All the models were painted with lacquer and sanded with No. 400 carborundum paper until aerodynamically smooth surfaces were obtained. The ordinates of the airfoil sections are presented in table I. Complete descriptions of these airfoil sections, including the methods of derivation and theoretical-pressure-distribution data, are available in reference 1.

Tests.—Lift and drag measurements were made for each smooth airfoil at Reynolds numbers of 15.0×10^6, 20.0×10^6, and 25.0×10^6 with the exception of the NACA 63_3–018 airfoil, which was tested only at Reynolds numbers of 15.0×10^6 and 20.0×10^6. Tank pressures were regulated so that Mach number effects would be negligible. In addition, the lift of the NACA 63–009 airfoil with a $0.20c$ simulated split flap deflected 60° was measured at Reynolds numbers of 9.0×10^6, 15.0×10^6, 20.0×10^6, and 25.0×10^6. The lift and drag characteristics of the plain NACA 63–009 airfoil with a roughened leading edge were also determined at the three higher Reynolds numbers. The standard roughness employed consisted of 0.011-inch carborundum grains secured with a light coat of shellac over a surface length of 8 percent of the chord back from the leading edge on the upper and lower surfaces of the airfoil. The grains were thinly spread to cover from 5 to 10 percent of this area.

RESULTS

The basic data obtained in the present investigation for the different airfoils are presented in the form of standard lift and drag coefficients in figures 1 to 9 for Reynolds numbers of 15.0×10^6, 20.0×10^6, and 25.0×10^6 together with data for Reynolds numbers of 3.0×10^6, 6.0×10^6, and 9.0×10^6 taken from reference 1. In order to facilitate the analysis of the effects of variations in the Reynolds number upon the aerodynamic characteristics and the manner in which these variations are affected by airfoil design, some of the important aerodynamic characteristics of each section have been plotted against Reynolds number in figures 10 to 12. Compensation for tunnel-wall effects has been made by the application of test-data corrections as explained in reference 2.

DISCUSSION

Since scale effects are the result of changing boundary-layer conditions, any explanation of these effects must necessarily be based upon the variation of boundary-layer structure and action with Reynolds number. The exact extent and nature of these changes are not readily predictable from the amount and type of data obtained in the present investigation. Through a consideration of accepted boundary-layer knowledge, however, a qualitative explanation of the test results is presented in terms of boundary-layer phenomena. Of more general interest to the designer is the selection of an airfoil suitable for a particular practical

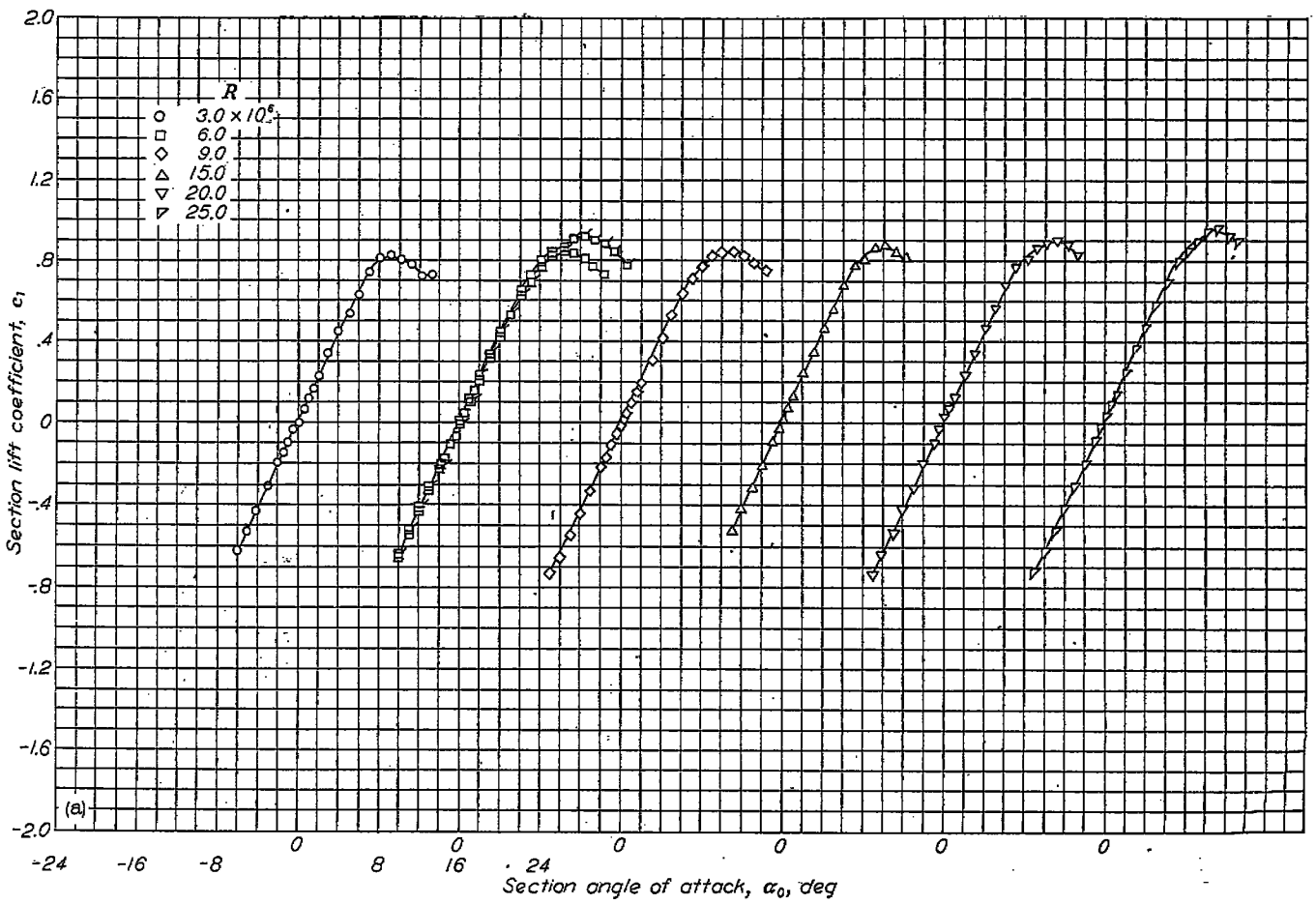

(a) Lift characteristics.

FIGURE 1.—Aerodynamic characteristics of the NACA 63-006 airfoil section. Flagged symbols denote leading-edge roughness.

application. With this purpose in mind, an attempt is made in the analysis to give some indication of the variations in scale effect that arise from changing the basic airfoil design parameters of thickness, thickness form, and camber.

DRAG

Minimum drag.—The reaction of the minimum drag coefficient of smooth airfoils to increasing Reynolds number, shown in figure 10, is attributed to the relative strengths of two interacting boundary-layer changes. A thinning of the boundary layer with increasing Reynolds number gives a gradual decrease of minimum drag. As the Reynolds number is increased beyond a certain value, however, the transition point begins to move forward and the drag increases. The initial decrease of minimum drag with increasing Reynolds number, shown by the data for some of the smooth airfoils, indicates that boundary-layer thinning is the predominant action taking place at the lower Reynolds numbers. The subsequent flattening of the scale-effect curves reveals the region where the transition of the boundary layer is beginning to move forward. The final rapid increase in minimum drag with Reynolds number increase indicates that forward movement of transition is the controlling factor.

Although these general trends are shown by the data for all the airfoils, the Reynolds numbers at which the different effects predominate depend somewhat on airfoil design. Some idea of the effect of thickness ratio upon the manner in which the minimum drag varies with Reynolds number may be gained by a comparison of the data for the NACA 63-series symmetrical sections having thicknesses from 6 percent to 18 percent chord, presented in figure 10 (a). The flat portions of the drag-scale-effect curves for the 6-percent-thick and 9-percent-thick sections show that in the Reynolds number range between 3.0×10^6 and approximately 10.0×10^6 the boundary-layer thinning and transition movement are approximately balanced with respect to their opposing tendencies to change the minimum drag. Increasing the Reynolds number for these sections beyond 10.0×10^6 brings about the predominance of the forward-moving transition region, as shown by the increase of minimum drag. The results for the airfoils of 12 percent thickness and 18 percent thickness show a gradual decrease of the minimum drag coefficient with Reynolds number within that range where the drag remained practically constant for the thinner sections. This decrease continues up to a Reynolds number of 10.0×10^6 for the 12-percent-thick section and up to 15.0×10^6 for the NACA 63_3–018 airfoil, after which the drag increases with further increase in Reynolds number.

As contrasted to the thinner airfoils, the flow conditions of the thicker airfoils are seen to be more favorable for delaying the forward movement of transition. An inspection of

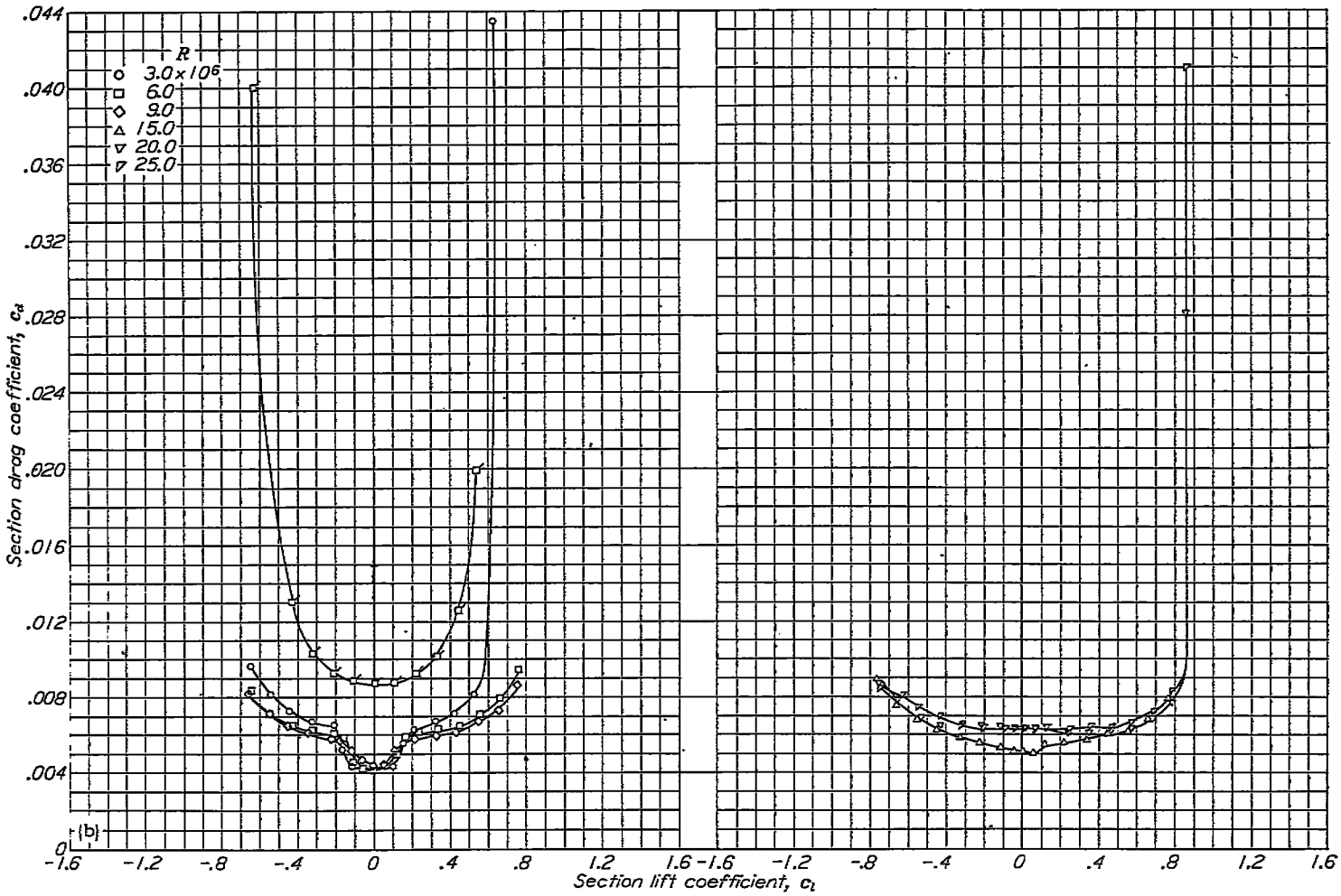

(b) Drag characteristics.

FIGURE 1.—Concluded.

the pressure distributions (reference 1) for the sections considered in the thickness variation shows that as the thickness increases the negative pressure gradient over the forward part of the airfoil becomes more negative. The influence of the airfoil pressure distribution upon the movement of the transition point with Reynolds number has been investigated by Schlichting and Ulrich (reference 3). The results of this work show the existence of a critical boundary-layer Reynolds number $R_{s_{cr}}$ above which the laminar layer is no longer stable and may become turbulent. Furthermore, the value of the critical boundary-layer Reynolds number is shown to increase rapidly and the laminar boundary layer, to become increasingly stable as the pressure gradient along the surface becomes more negative. The greater negative pressure gradients of the 12-percent-thick and 18-percent-thick sections are probably responsible for a delay in the Reynolds number at which transition moves forward and, hence, a net drag reduction is noticeable for the thick sections up to fairly high values of the Reynolds number.

Because of the manner in which the character of the drag-scale-effect curves varies with airfoil thickness, the minimum drag coefficient shows a trend toward decreasing with increasing airfoil thickness within the range of Reynolds number between 15.0×10^6 and 25.0×10^6. The trend is not entirely consistent, and it cannot be assumed that any advantage can be retained by the thicker sections as the value of the Reynolds number is increased beyond those considered in this investigation. The results of tests made on these same sections with standard leading-edge roughness have been correlated to give the variation of minimum drag with thickness ratio at a Reynolds number of 6.0×10^6 (reference 1). These results, which correspond to fully developed turbulent boundary layers on the airfoil surfaces, show that the minimum drag increases fairly rapidly as the thickness of the section is increased. The fact that the drag at a Reynolds number of 25.0×10^6 is approximately the same for the smooth airfoils of different thicknesses would seem to indicate a variation in the relative extent of turbulent flow on the different airfoils. If such is the case, increasing the Reynolds number beyond 25.0×10^6 to a value at which fully developed turbulent layers exist on the surfaces of all the airfoils would presumably result in minimum drag coefficients which increase with airfoil thickness ratio.

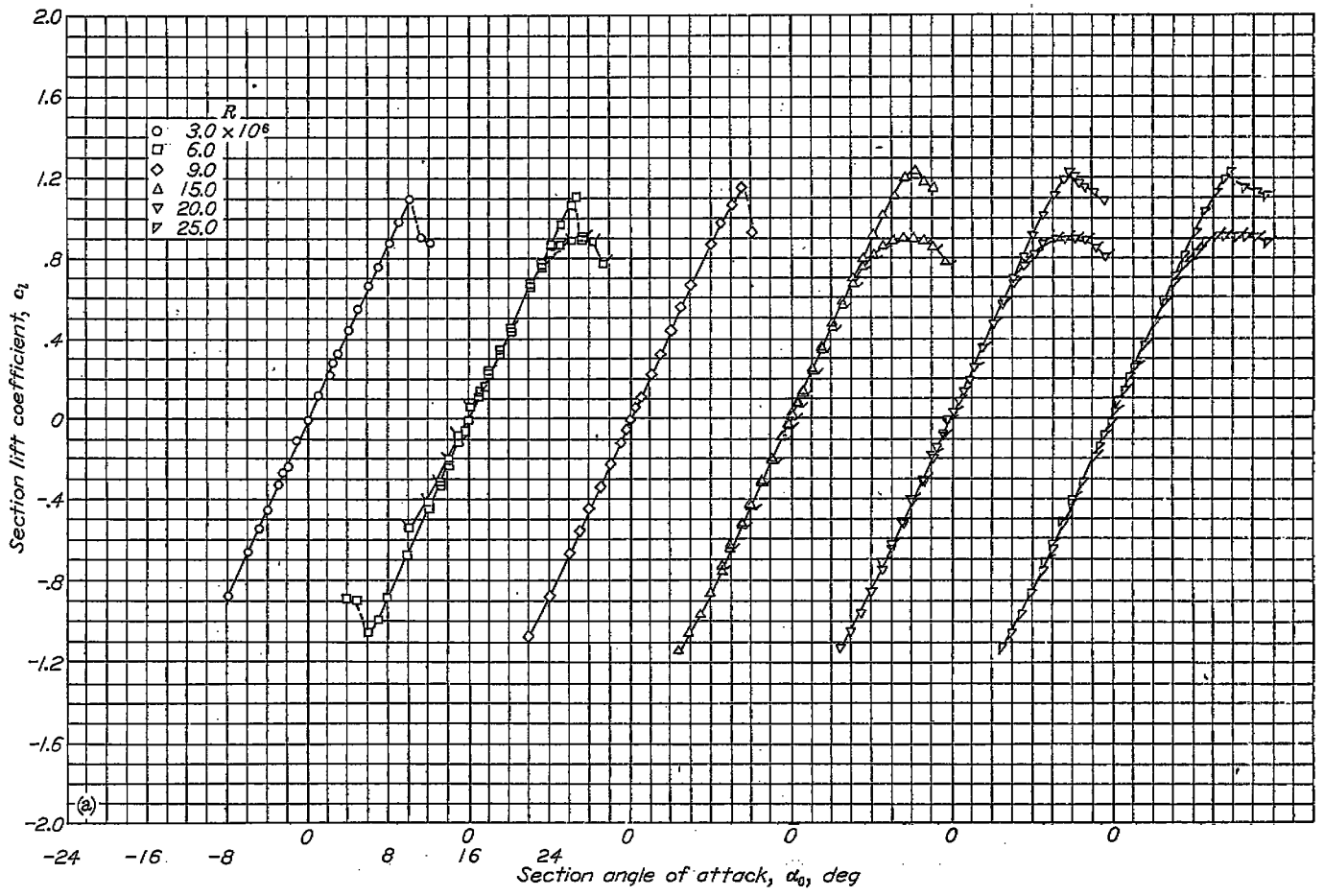

(a) Lift characteristics.

FIGURE 2.—Aerodynamic characteristics of the NACA 63-009 airfoil section. Flagged symbols denote leading-edge roughness.

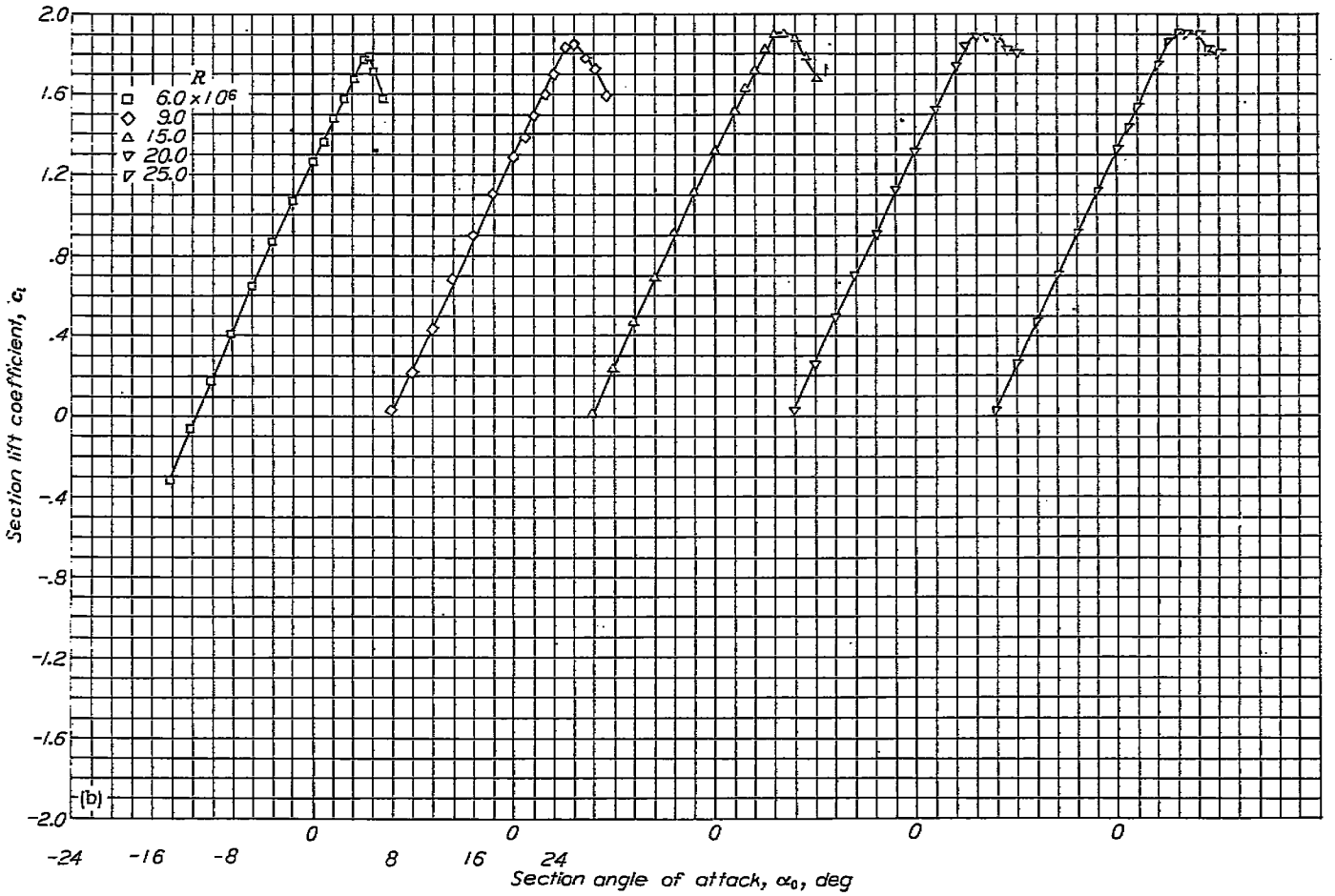

(b) Lift characteristics with 0.20c simulated split flap deflected 60°.

FIGURE 2.—Continued.

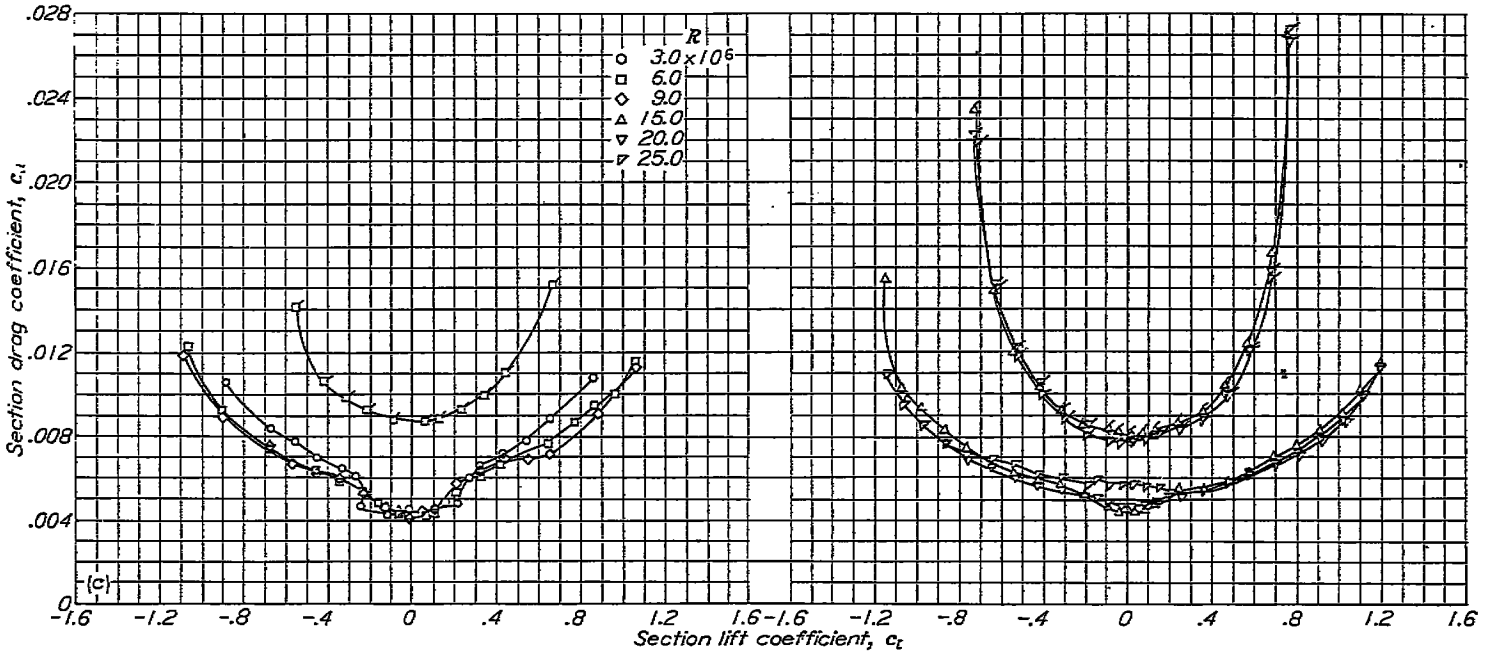

(c) Drag characteristics.

FIGURE 2.—Concluded.

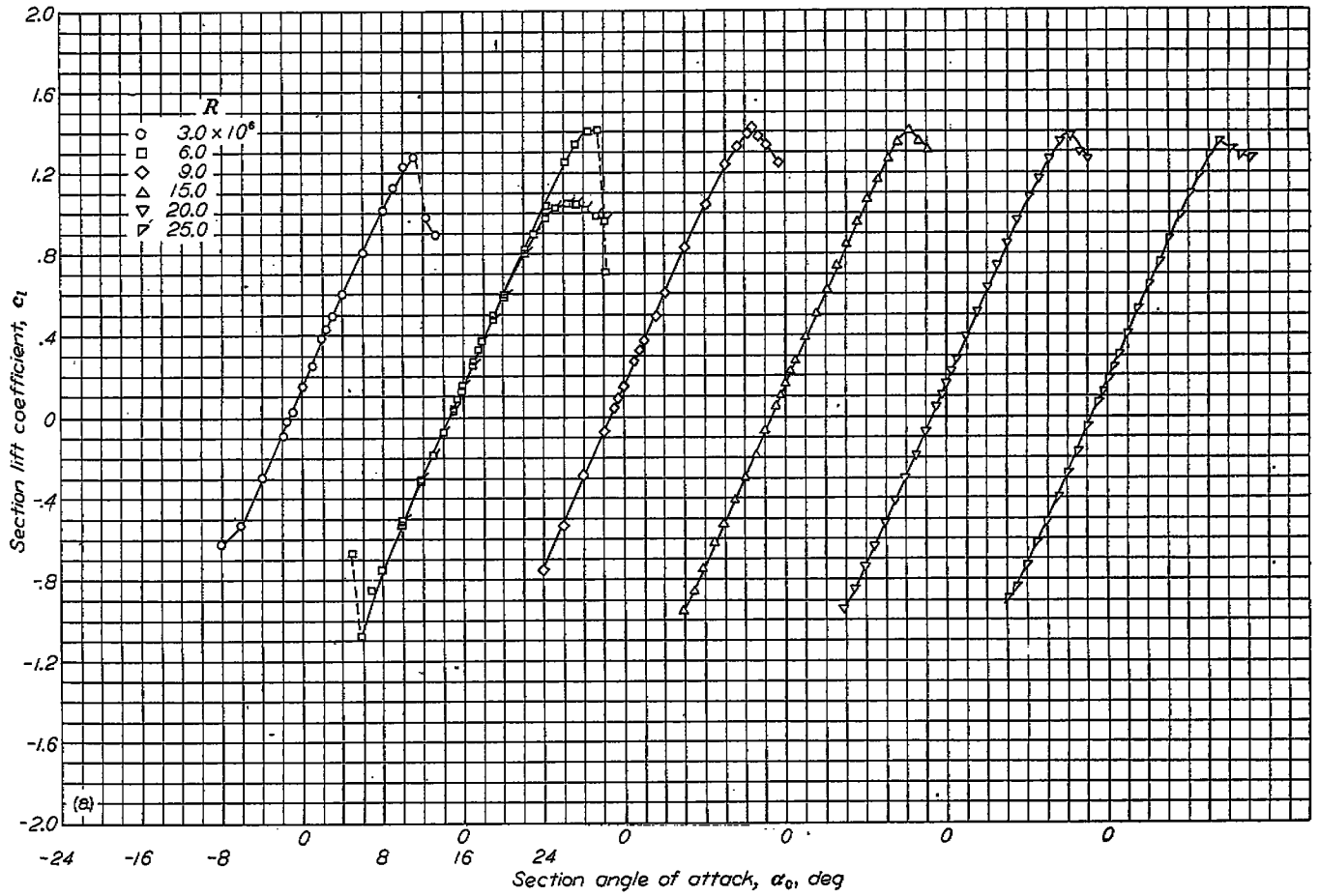

(a) Lift characteristics.

FIGURE 3.—Aerodynamic characteristics of the NACA 63-209 airfoil section. Flagged symbols denote leading-edge roughness.

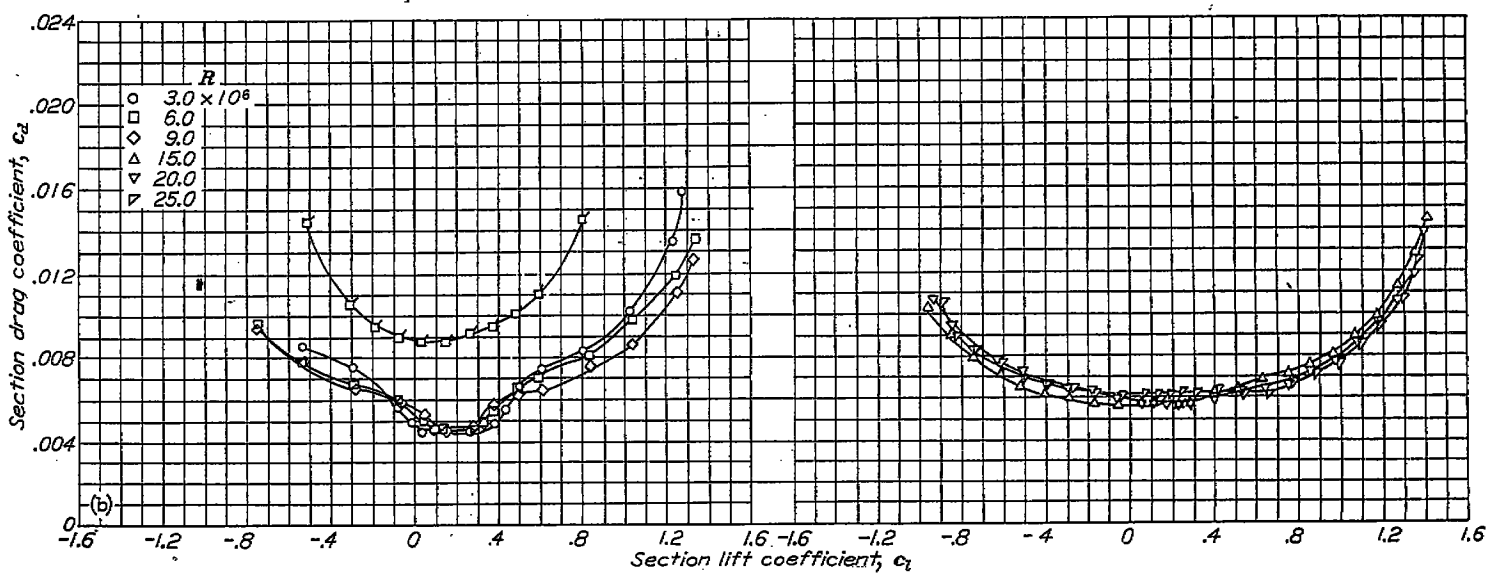

(b) Drag characteristics.

FIGURE 3.—Concluded.

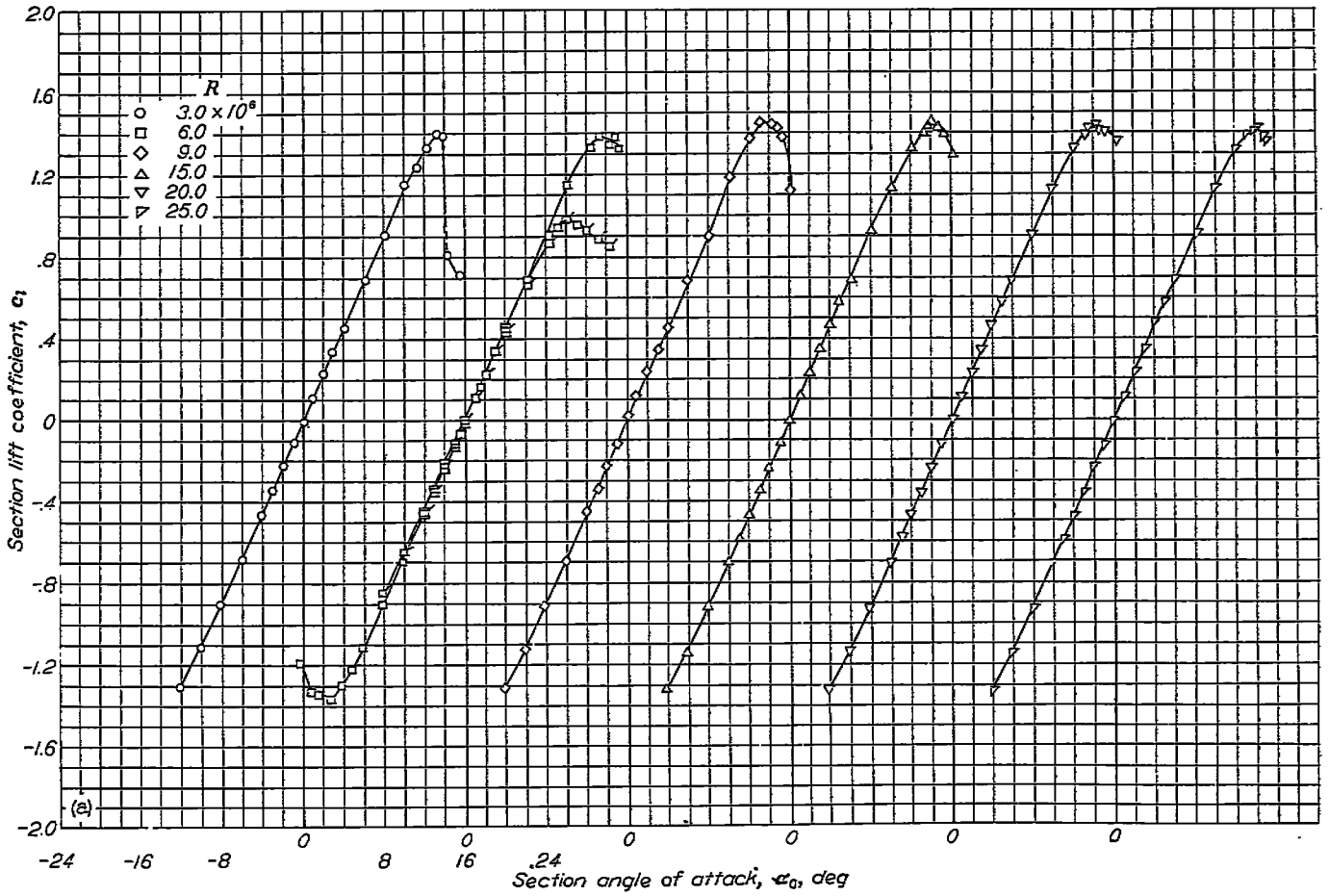

(a) Lift characteristics.

FIGURE 4.—Aerodynamic characteristics of the NACA 63_1-012 airfoil section. Flagged symbols denote leading-edge roughness.

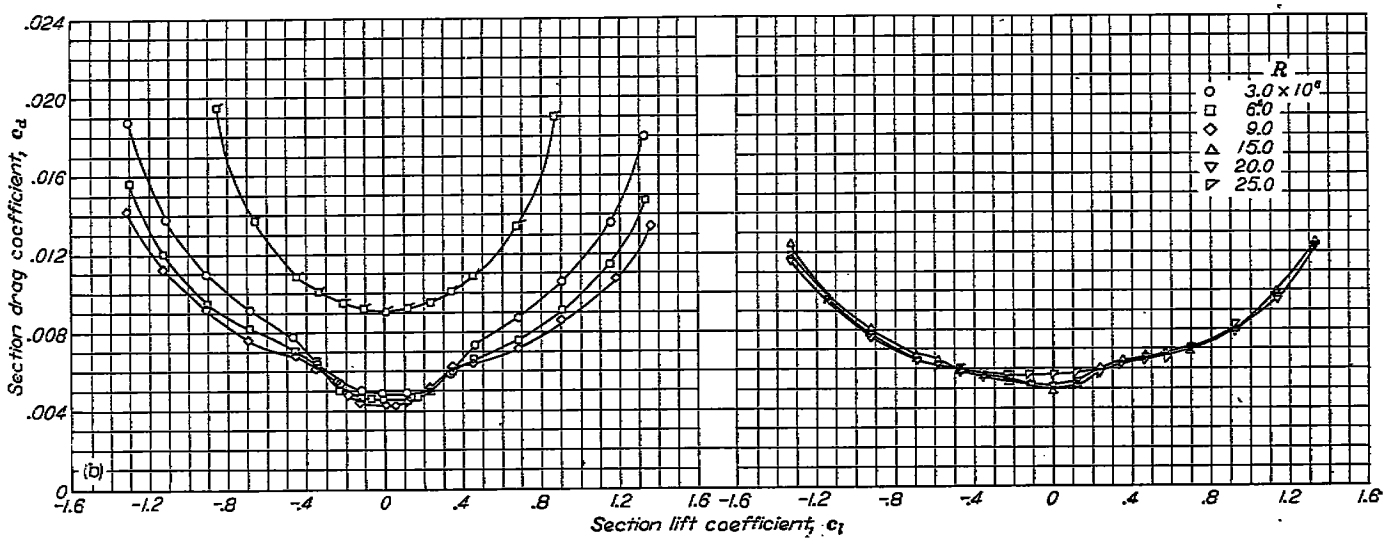

(b) Drag characteristics.

FIGURE 4.—Concluded.

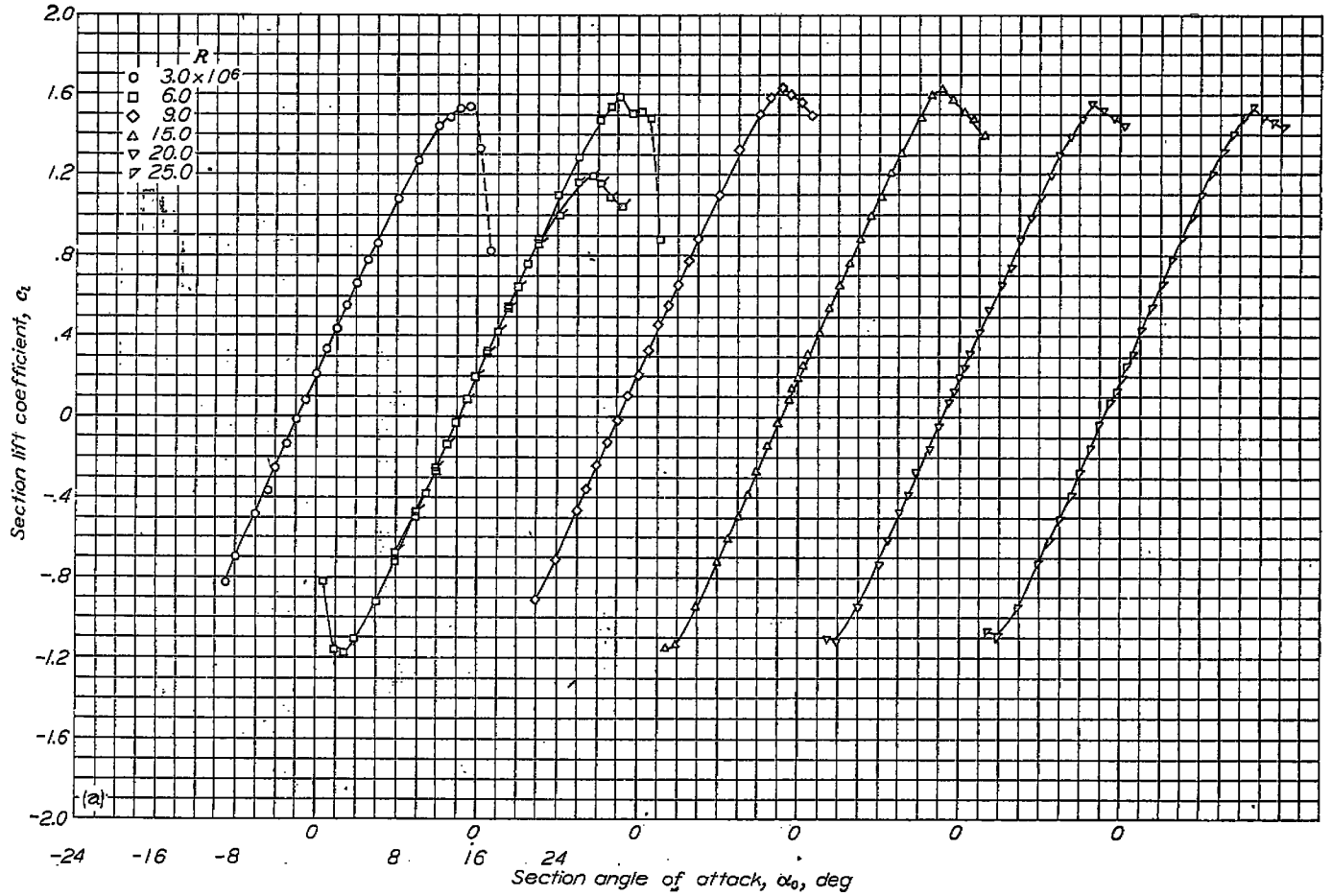

(a) Lift characteristics.

FIGURE 5.—Aerodynamic characteristics of the NACA 63$_1$-212 airfoil section. Flagged symbols denote leading-edge roughness.

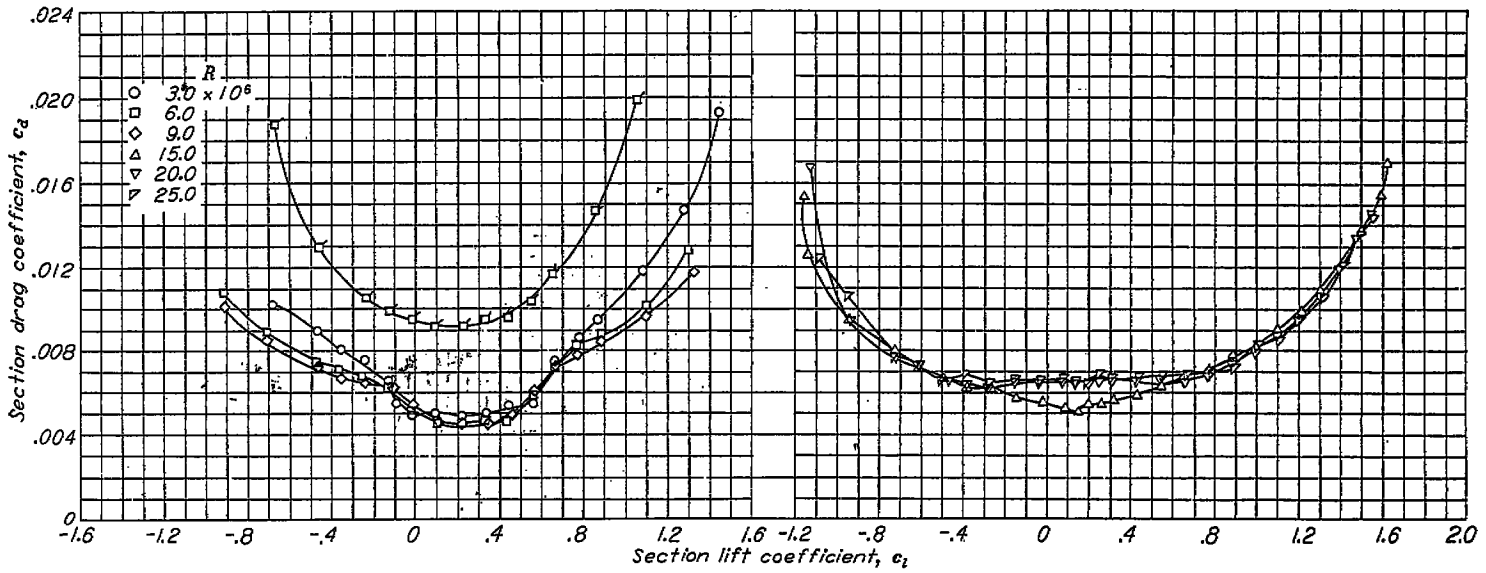

(b) Drag characteristics.

FIGURE 5.—Concluded.

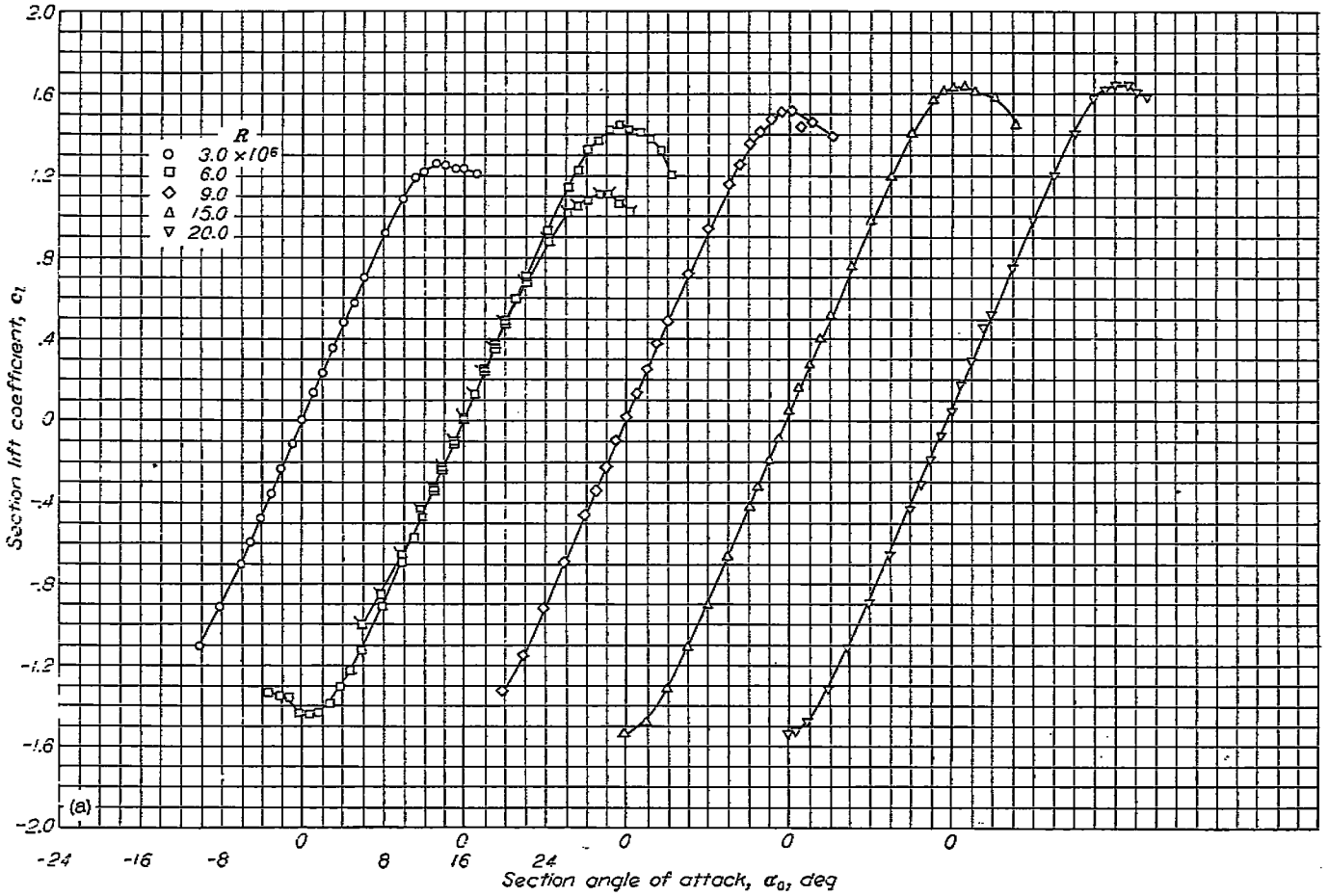

(a) Lift characteristics.

FIGURE 6.—Aerodynamic characteristics of the NACA 63₃-018 airfoil section. Flagged symbols denote leading-edge roughness.

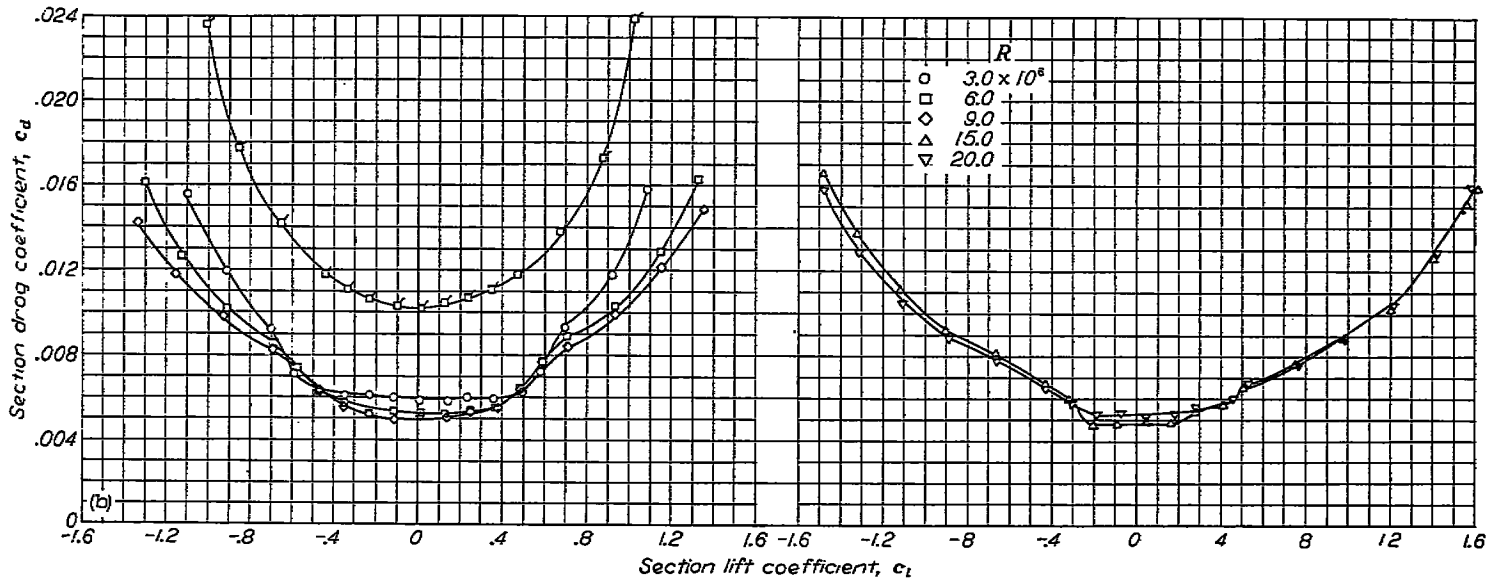

(b) Drag characteristics.

FIGURE 6.—Concluded.

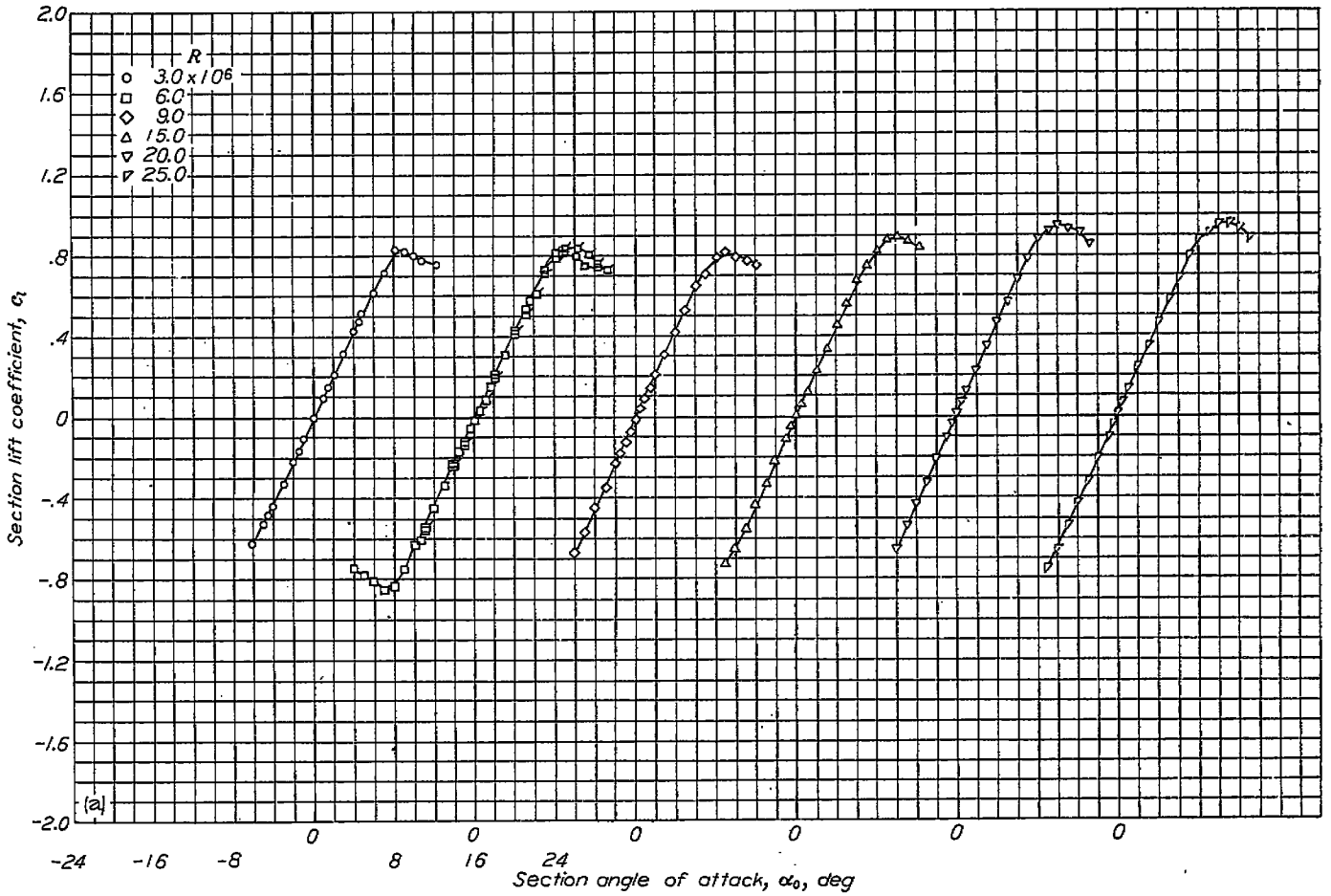

(a) Lift characteristics.

FIGURE 7.—Aerodynamic characteristics of the NACA 64-006 airfoil section. Flagged symbols denote leading-edge roughness.

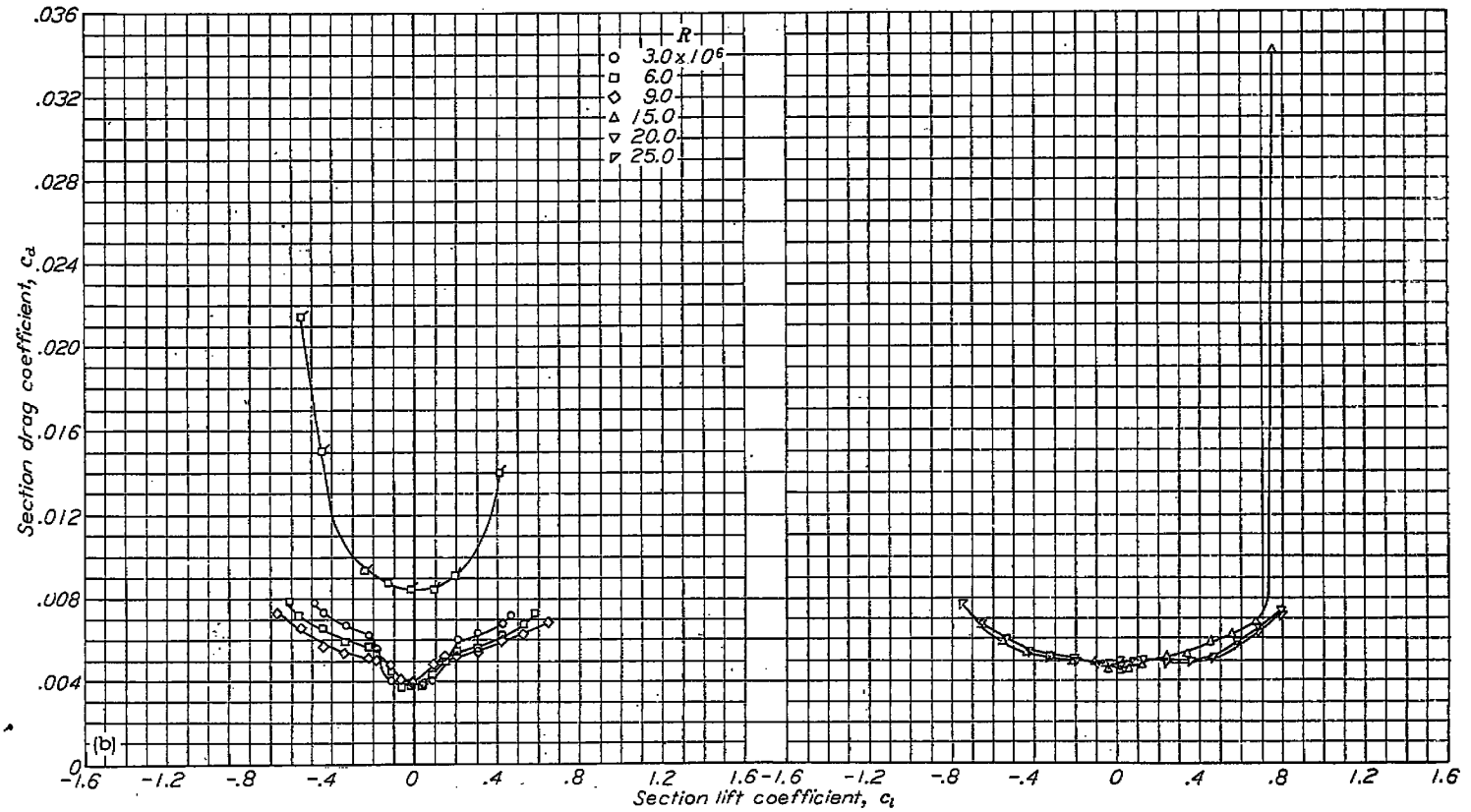

(b) Drag characteristics.

FIGURE 7.—Concluded.

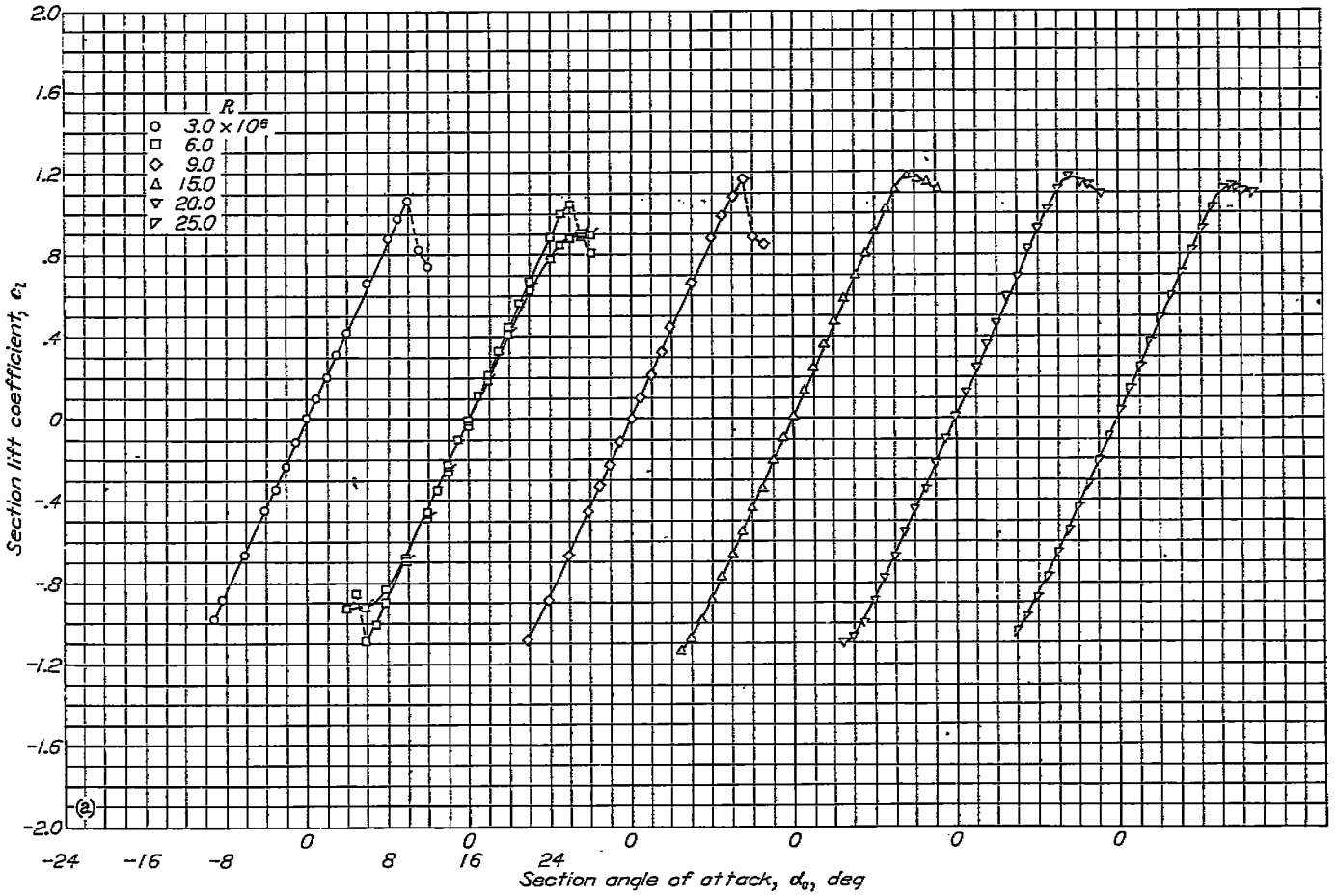

(a) Lift characteristics.

FIGURE 8.—Aerodynamic characteristics of the NACA 64-009 airfoil section. Flagged symbols denote leading-edge roughness.

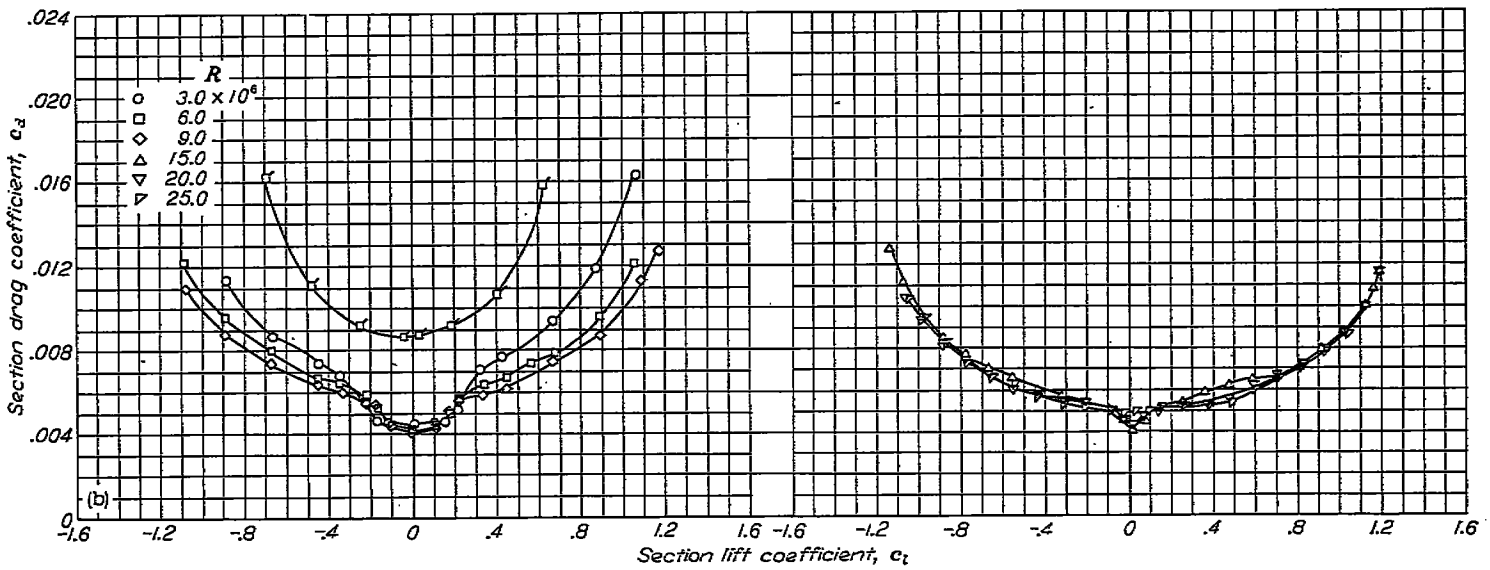

(b) Drag characteristics.

FIGURE 8.—Concluded.

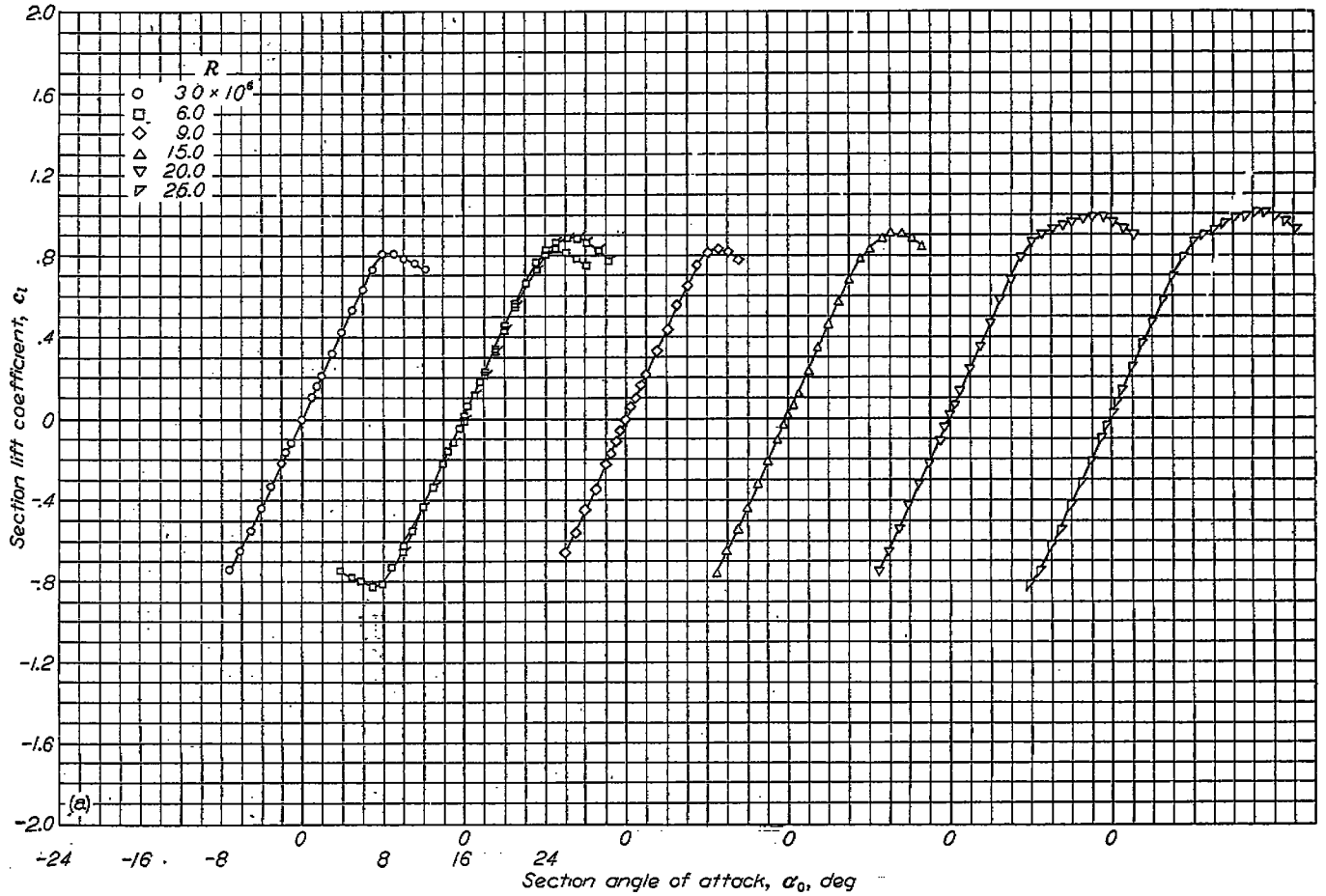

(a) Lift characteristics.

FIGURE 9.—Aerodynamic characteristics of the NACA 65-006 airfoil section. Flagged symbols denote leading-edge roughness.

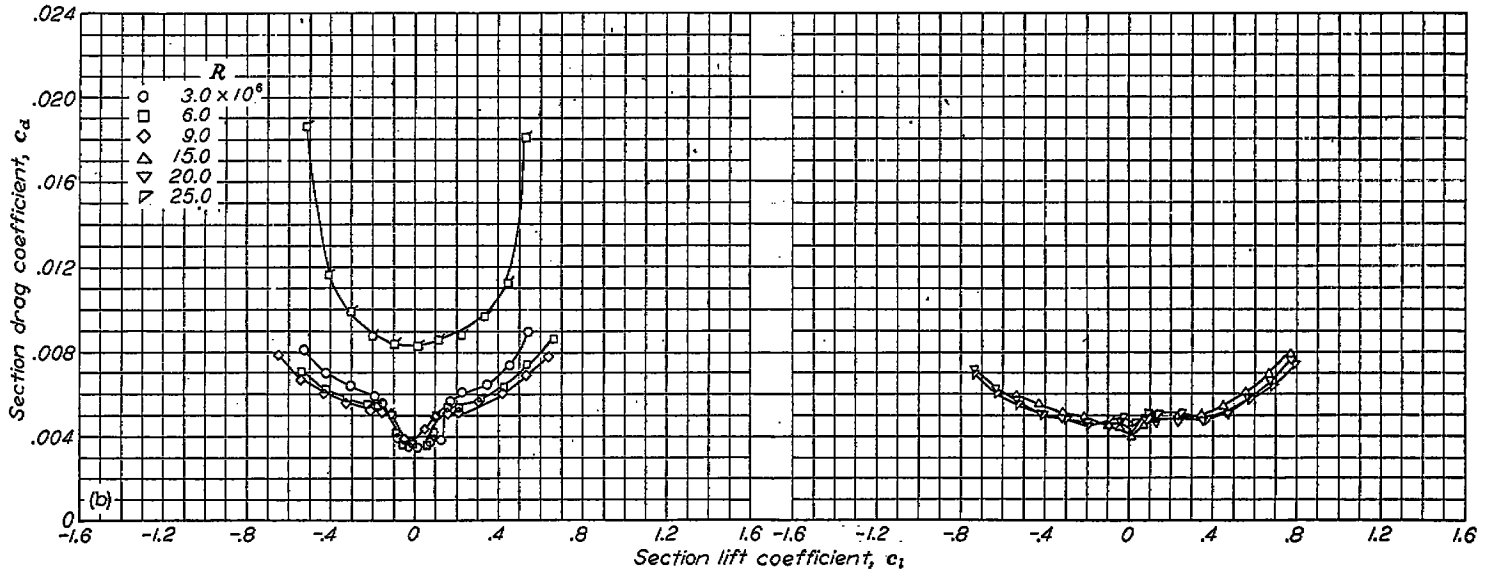

(b) Drag characteristics.

FIGURE 9.—Concluded.

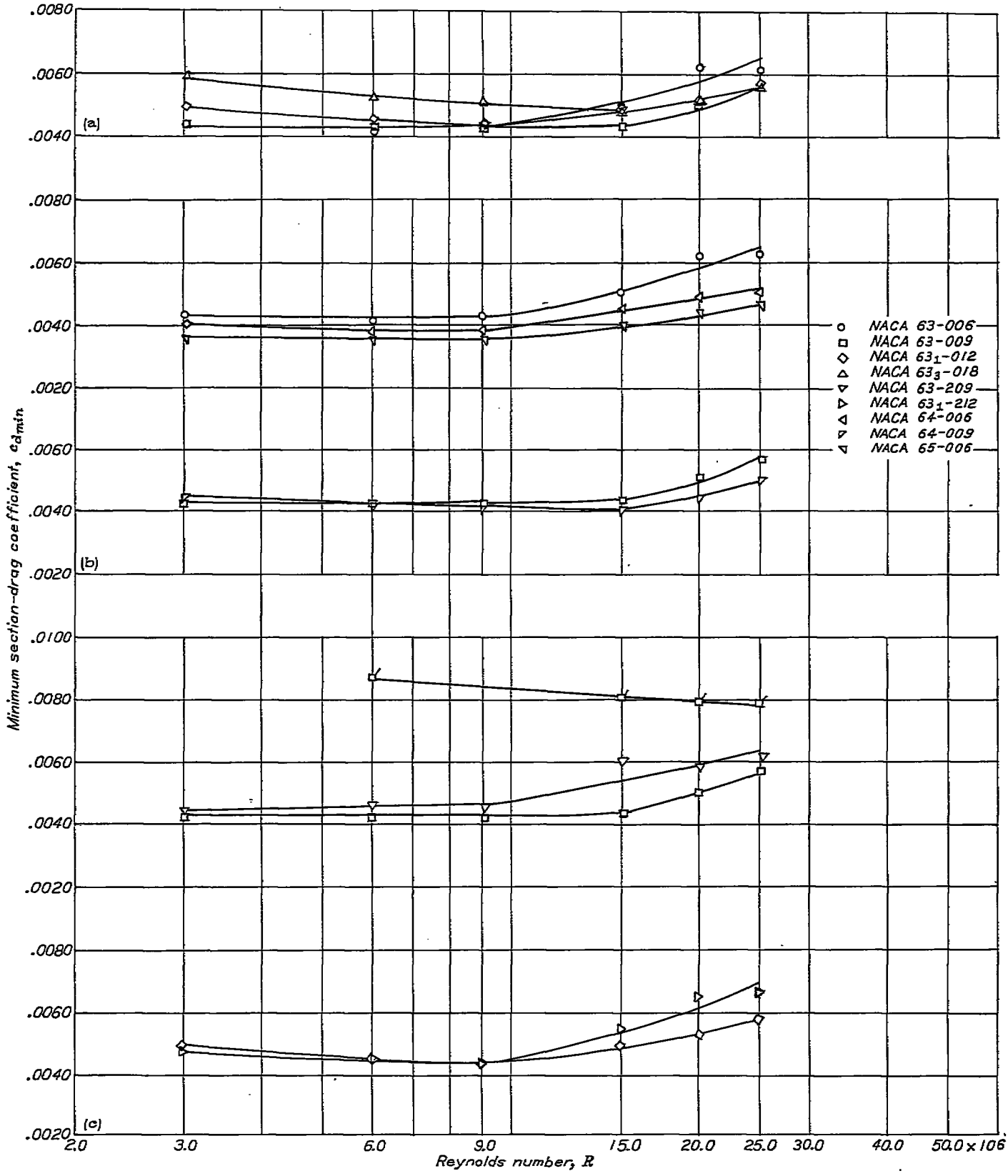

(a) Effect of thickness.
(b) Effect of thickness form.
(c) Effect of camber.

FIGURE 10.—Variation of section minimum drag coefficient with Reynolds number for nine NACA 6-series airfoils of varying thickness, thickness form, and camber. Flagged symbols denote leading-edge roughness.

The greater extent of the laminar boundary layer which results as the point of minimum pressure is moved rearward is evidenced by the progressively lower minimum drag coefficients of the NACA 63–006, NACA 64–006, and NACA 65–006 airfoil sections at a Reynolds number of 3.0×10^6 (fig. 10 (b)). In general, moving the point of minimum pressure rearward has little effect on the sequence in which the boundary-layer effects occur. The values of the drag coefficient for these airfoils appear to be relatively insensitive to variations in the Reynolds number until a Reynolds number of the order of 15.0×10^6 is exceeded. At higher Reynolds numbers, the rate of forward movement of transition appears to be reduced as the point of minimum pressure is moved from 30 percent to 40 percent chord. Further rearward movement of the position of minimum pressure has little effect on the rate of the forward movement of transition, at least for these thin airfoils. The data for the 9-percent-thick 63-series and 64-series airfoils show the same trends.

An inspection of figure 10 (c) shows that the addition of a small amount of camber to the 9-percent-thick and 12-percent-thick 63-series sections does not have any consistent effect upon the value of the minimum drag between Reynolds numbers of 3.0×10^6 and 9.0×10^6. Increases in the Reynolds number beyond 9.0×10^6, however, appear to cause more rapid forward movement of transition for the cambered airfoils than for the symmetrical airfoils. Only two cambered sections were tested, however, and this trend is therefore not very well established.

The addition of standard roughness to the NACA 63–009 section (fig. 10 (c)) causes a large increase in the minimum drag at all Reynolds numbers, but increasing the Reynolds number has a favorable effect in reducing the drag. These results are to be expected from a consideration of boundary-layer theory for a fully developed turbulent boundary layer. (See reference 4.)

Low-drag range.—Increasing the Reynolds number from 9.0×10^6 to 15.0×10^6 resulted in the almost complete disappearance of the low-drag range of all the airfoils except that of 18 percent thickness (figs. 1 to 9). The previously discussed predominating influence of forward movement of transition at the higher Reynolds numbers, together with the influence of pressure gradient upon the Reynolds number at which this forward movement begins to predominate, explains these drag results.

Drag data outside the low-drag range.—The drag polars for the different airfoils (figs. 1 to 9) indicate that, for a given lift coefficient outside the low-drag range, the drag decreases as the Reynolds number is varied from 3.0×10^6 to 9.0×10^6. Further increases in the Reynolds number, however, do not seem to have any appreciable effect upon the drag. Variations in the airfoil design parameters appear to have no consistent influence upon the effect of Reynolds number on the drag outside the low-drag range. Although roughness increases the drag greatly in this region, the value of the drag for the rough-surface condition seems to be relatively insensitive to Reynolds number as shown by the data for the NACA 63–009 section (fig. 2).

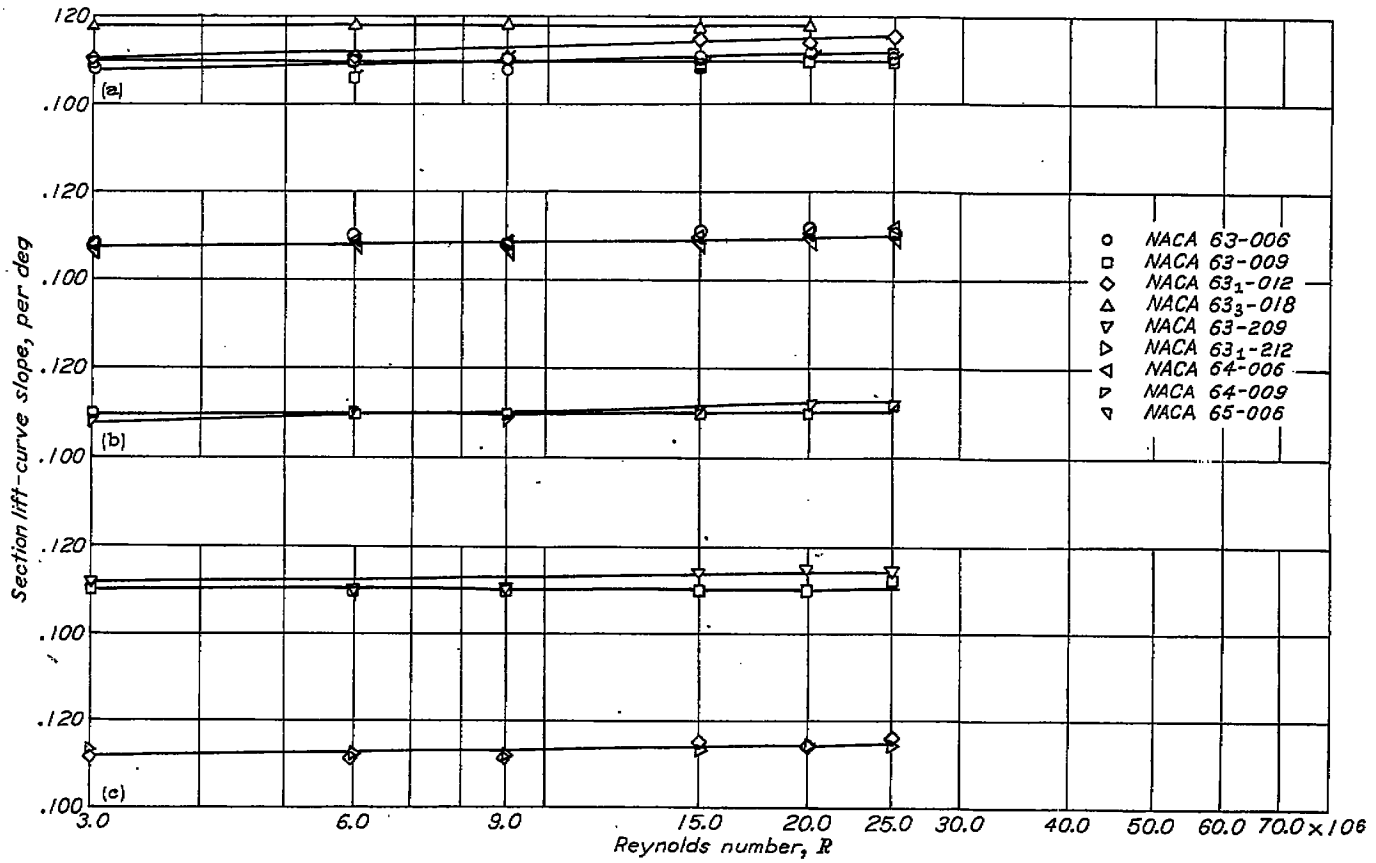

(a) Effect of thickness.
(b) Effect of thickness form.
(c) Effect of camber.

FIGURE 11.—Variation of section lift-curve slope with Reynolds number for nine NACA 6-series airfoils of varying thickness, thickness form, and camber. Flagged symbols denote leading-edge roughness.

LIFT

The important characteristics associated with the lift curve are the angle of zero lift, lift-curve slope, and the maximum lift coefficient. In order to facilitate the analysis of lift data presented in figures 1 to 9, values of these parameters were determined from the test data at the six Reynolds numbers between 3.0×10^6 and 25.0×10^6. The values of the angle of zero lift of the cambered airfoils showed almost no variation with Reynolds number and, therefore, are not presented as a cross plot against Reynolds number. The values of the section lift-curve slope and maximum section lift coefficient are presented as functions of Reynolds number in figures 11 and 12.

Lift-curve slope.—The lift-curve slopes were obtained from the best representative straight line through the experimental-data points in the angle-of-attack range of 4°

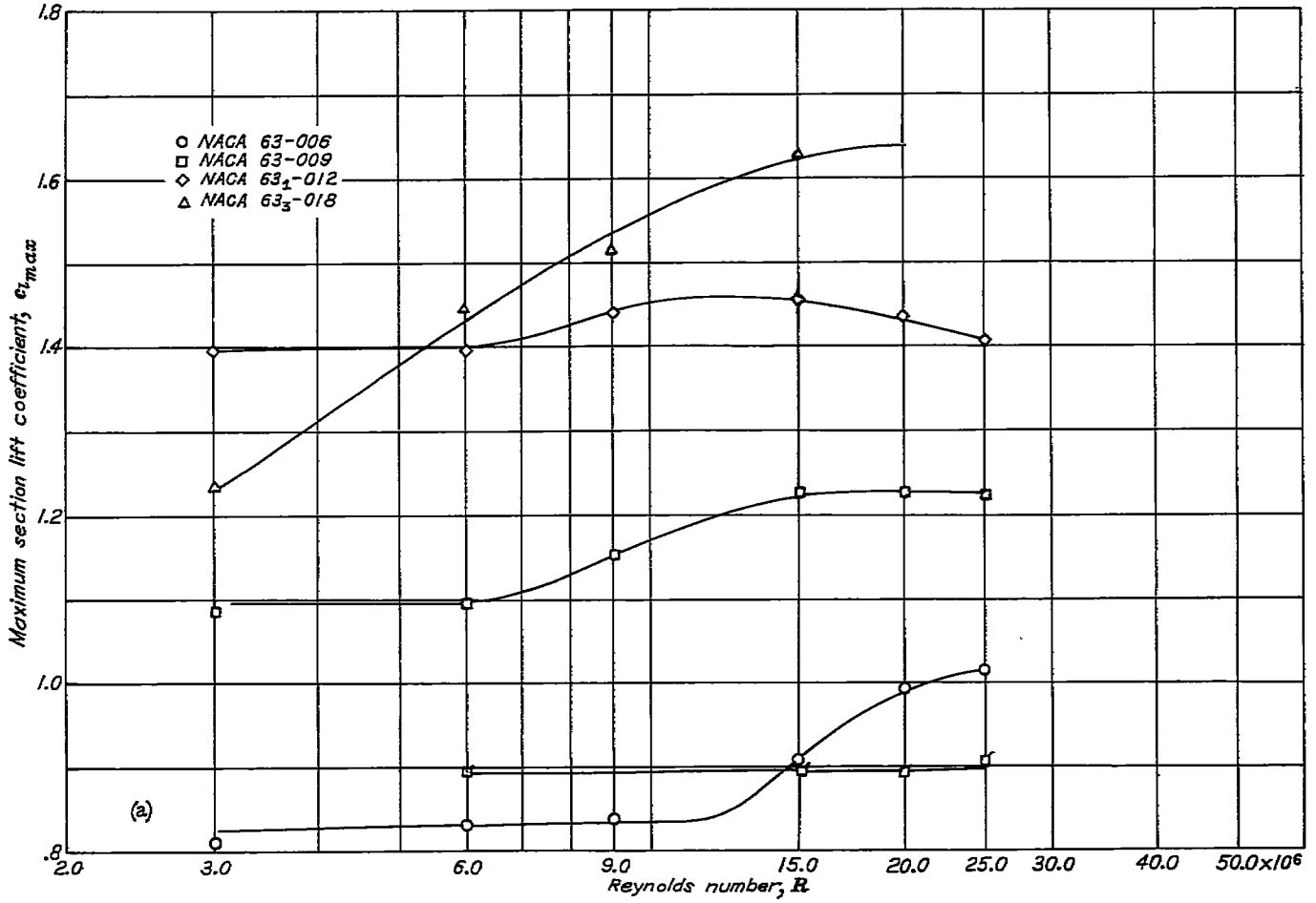

(a) Effect of thickness.

FIGURE 12.—Variation of maximum section lift coefficient with Reynolds number for nine NACA 6-series airfoils of varying thickness, thickness form, and camber. Flagged symbols denote leading-edge roughness.

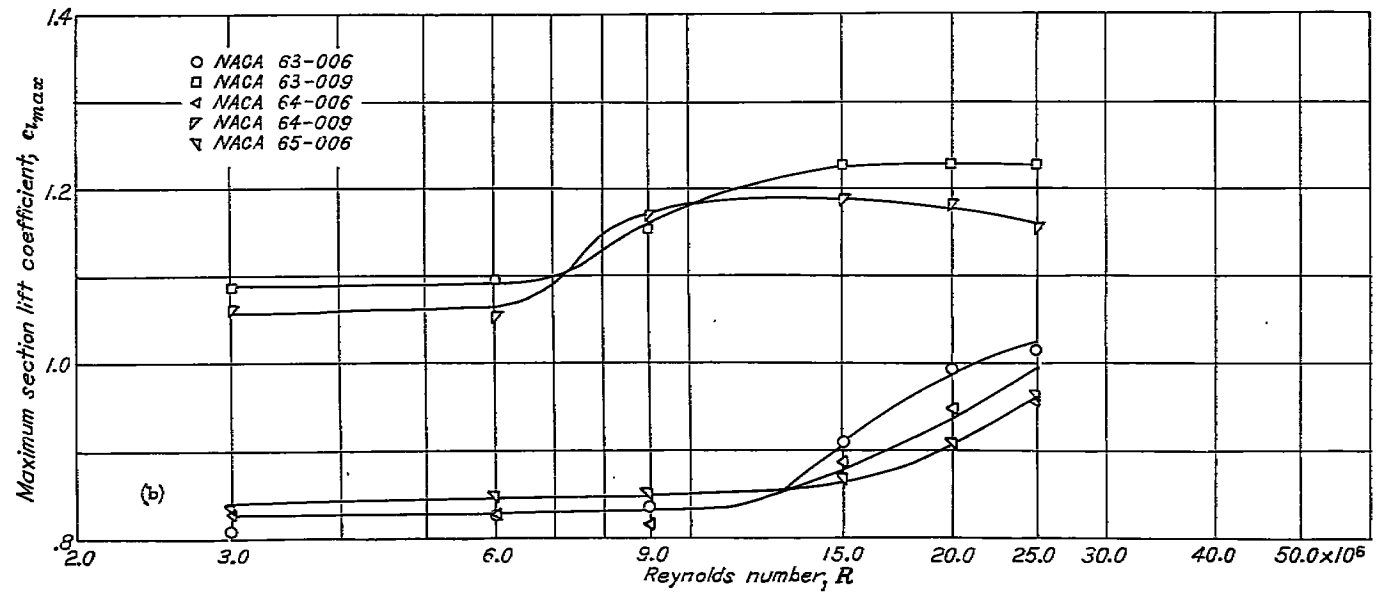

(b) Effect of thickness form.

FIGURE 12.—Continued.

on each side of the design lift coefficient. Throughout the range of Reynolds number of this investigation, the values of the lift-curve slope (fig. 11) for the smooth sections tested are very close to that predicted by thin-airfoil theory (2π per radian or 0.110 per degree). The lift-curve slopes of some of the sections show a slight tendency to increase with Reynolds number but, for design purposes, this slight effect is probably unimportant. For the airfoils under consideration, the section lift-curve slope varies only slightly with the airfoil thickness form but increases with thickness. This trend was noted in the data of reference 1 for all NACA 6-series airfoils. The addition of leading-edge roughness to the NACA 63–009 section does not affect appreciably the section lift-curve slope in the range of Reynolds number of this investigation. This result should not, however, be taken to apply to airfoils of all thickness ratios. The data of reference 1 show the values of the lift-curve slope of the smooth and rough airfoils to diverge appreciably as the thickness ratio is increased above 10 to 12 percent. These data are for a Reynolds number of 6.0×10^6 but a somewhat similar trend might be expected at higher Reynolds numbers.

Maximum lift.—The effects on the maximum lift of increase in the Reynolds number from 3.0×10^6 to 25.0×10^6 follow either of two general trends, depending upon the order of magnitude of the airfoil thickness ratio (fig. 12). For airfoils of 12 percent thickness or less, the maximum lift remains relatively constant over the lower range of Reynolds number. Extending the Reynolds number beyond this range, however, causes a rapid increase followed by a leveling off or slight decrease of the maximum lift. The results obtained for the 18-percent-thick section, however, show an entirely different type of scale effect as evidenced by a relatively steady increase in maximum lift over the Reynolds number range.

The detailed differences in the flow mechanism responsible for the observed differences in the type of scale effect shown by the thick and thin sections are not entirely clear. Unpublished data at a Reynolds number of 6.0×10^6 show that 63-series airfoils, of 12 percent thickness and less, stall as a result of abrupt laminar separation of the flow near the leading edge, whereas 63-series airfoils of 18 percent thickness stall as a result of a gradual separation of the turbulent layer moving forward from the trailing edge. By the use of these results as a starting point, a qualitative flow mechanism can be traced which offers a possible explanation for the type of scale effect shown by the thick and thin sections. The basic ideas presented in the following discussion of the flow mechanism are those of Jacobs and Sherman (reference 5) in a somewhat extended form.

Consider first the airfoils of 12 percent thickness or less which are known to stall as a result of laminar separation at

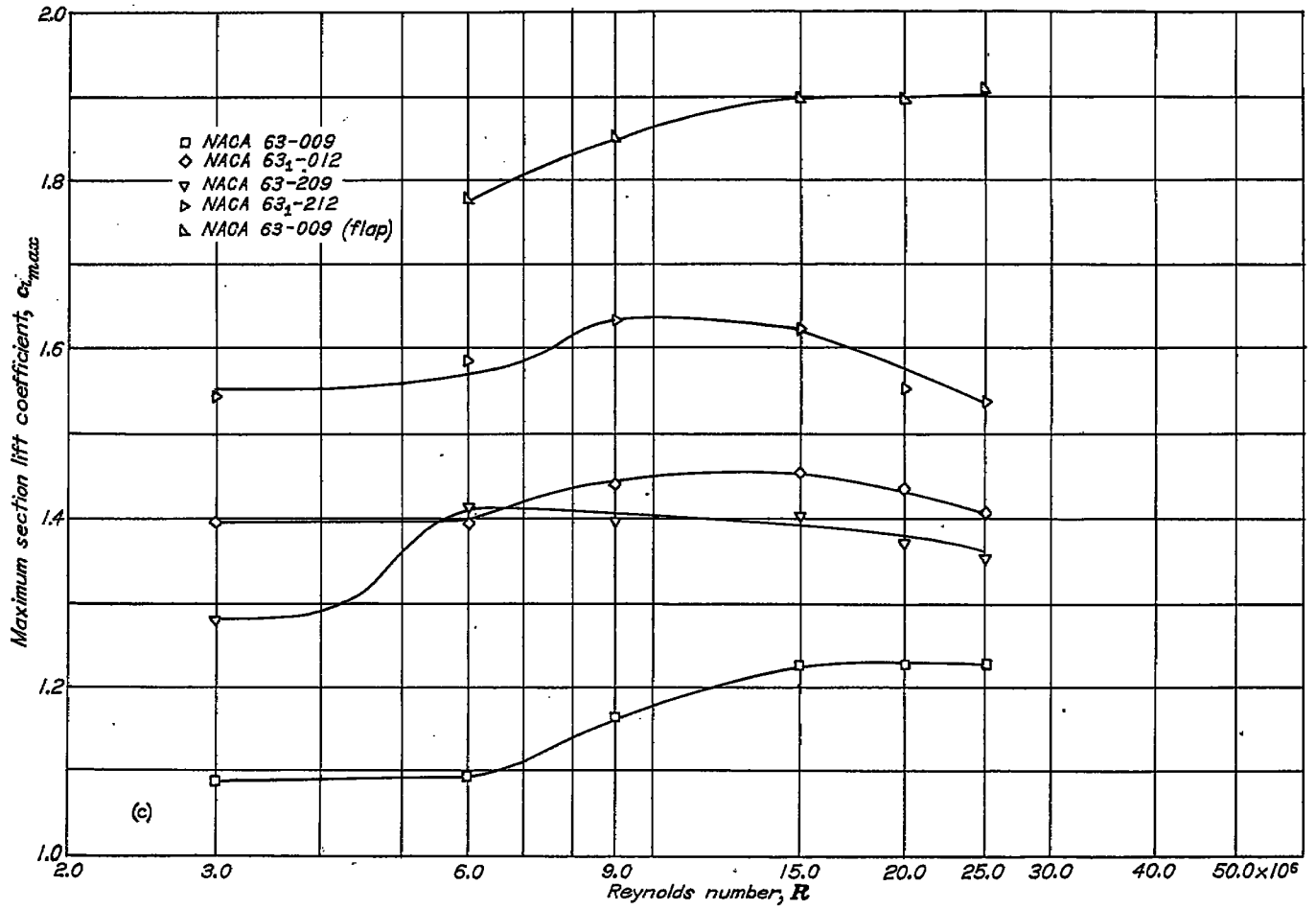

(c) Effect of camber.

FIGURE 12.—Concluded.

the leading edge. The point at which laminar separation occurs and the magnitude of the pressure recovery which may be withstood before the laminar layer separates are not influenced by the value of the Reynolds number. For airfoils which stall by separation of the laminar layer near the leading edge, the Reynolds number would not, therefore, be expected to have any effect upon the maximum lift if the possibility of the separated layer reattaching itself to the surface were disregarded. Since the data of figure 12 show no scale effect on the maximum lift of the thin airfoils over the lower range of Reynolds number and since these airfoils are known to stall by laminar separation within this range, it might be assumed that, once the flow is completely separated, increasing the Reynolds number does not result in its reattachment within this lower range of Reynolds number.

The subsequent rapid increase in maximum lift over a relatively short range of Reynolds number (fig. 12) is believed to indicate that the separated laminar layer is reattaching itself to the surface as a turbulent layer. Data showing such a reattachment with a "bubble" or "dead air" region existing between the points of laminar separation and turbulent reattachment are presented in references 6 and 7. These results also show that the bubble decreases in size as the Reynolds number is increased for an airfoil at a given angle of attack. A qualitative speculation is advanced in reference 6 as an explanation for the reattachment and decrease in size of the bubble with increasing Reynolds number under given conditions of pressure gradient. According to these ideas, a definite Reynolds number R' should exist between the point at which laminar separation occurs and the point of transition along the separated laminar layer at which turbulence begins. If the assumption is made that the turbulence spreads from the transition point at a given angle, reattachment will occur when this spreading turbulent flow strikes the surface and establishes itself as a turbulent boundary layer. For a given airfoil shape at a given angle of attack, increasing the wing Reynolds number will decrease the distance corresponding to the Reynolds number R' necessary for the separated laminar layer to break up into turbulence. The size of the bubble, therefore, decreases with increasing Reynolds number.

By application of the ideas just discussed to the phenomenon of laminar separation of the flow near the leading edge of an airfoil, the point of reattachment may be seen to depend upon the pressure gradient, the Reynolds number, and the curvature of the airfoil surface. Assume that the Reynolds number of one of the thin airfoils (fig. 12 (a)) is such that the flow just reattaches itself to the surface at an angle of attack corresponding to maximum lift at a somewhat lower Reynolds number. Increasing the angle of attack under such circumstances will have the following effects. The pressure gradient at the leading edge will become more adverse and the negative pressure peak, higher. The laminar separation point will then move forward around the curved leading edge of the airfoil. On the assumption that the separated laminar layer flows away from the surface in a direction tangential to the surface at the point of separation forward movement of the separation point has a definitely adverse effect upon the possibility of flow reattachment. On the other hand, because of the increased velocities over the surface, the linear distance corresponding to the Reynolds number R' required for turbulence to begin in the separated layer decreases, and this decrease has a favorable effect upon flow attachment. For a given angle of attack and bubble size, further increases in lift at the same Reynolds number would seem to depend upon the relative strength of these two effects. The data of figure 12 (a), which show the maximum lift of the thinner airfoils to increase rapidly over a relatively short range of Reynolds number, would seem to indicate that at a given angle of attack and depending upon the initial bubble size, which in turn depends upon the wing Reynolds number, appreciable increase in lift is possible before forward movement of separation becomes the predominant effect and causes the flow to separate permanently.

The preceding discussion is based on the assumption that maximum lift is a function only of phenomena occurring at the leading edge. The changes in the flow field near the leading edge, however, cannot be considered as affecting only local conditions at that point but must also be considered in relation to the flow over the rear of the airfoil. The decrease in size of the laminar-separation bubble near the leading edge has a beneficial effect upon the turbulent layer near the trailing edge. This beneficial effect depends on the fact that the initial conditions of the turbulent layer as it begins near the leading edge are so altered that more pressure recovery may be withstood before separation begins near the trailing edge. The increased negative pressure peaks near the leading edge which the decrease in size of the laminar-separation bubble permits, however, have a distinctly adverse effect upon the tendency of the turbulent layer to separate at the rear of the airfoil.

As the process of increasing maximum lift with increasing Reynolds number continues, a situation may be imagined in which the turbulent layer near the trailing edge becomes critical and starts to separate. The effect of this separation on the flow field around the airfoil is of the same type as that produced by the small negative deflection of a plain flap. The beginning of turbulent separation at the rear of the airfoil thus results in higher negative pressure peaks near the leading edge for a given lift coefficient (reference 8). The effect of these higher peaks is to increase the size of the laminar-separation bubble which, together with the higher pressure recoveries, tends to cause more turbulent separation at the rear of the airfoil. A regenerative process could thus be established which would quickly limit the maximum lift. Such a process is believed to be responsible for the experimentally observed fact (fig. 12 (a)) that the maximum lift of the thin airfoils, after a rapid rise over a relatively short range of Reynolds number, rather suddenly ceases to increase. A consideration of these ideas indicates that, even within that range of Reynolds number where laminar separation at the leading edge is known to limit the lift as in the first flat portion of the scale-effect curves (fig. 12 (a)), the tendency toward turbulent separation at the rear of the airfoil may have a controlling effect upon the observed phenomenon of laminar separation at the leading edge.

If the preceding discussion is assumed to depict a reasonably accurate qualitative picture of the mechanism by which maximum lift is reached at the upper end of that small range of Reynolds number over which the maximum lift increases rapidly, the lack of further appreciable scale effect would seem to indicate that separation of the turbulent layer is little affected by variations in the Reynolds number. The work of Von Doenhoff and Tetervin (reference 9) on turbulent separation indicates that, if the initial conditions of the turbulent layer are not altered, increasing the Reynolds number actually has a slightly adverse effect upon the amount of pressure recovery which may be withstood before turbulent separation occurs. The lack of adverse scale effect shown by most of the data of figure 12 (a) can possibly be explained by variations in the condition of the short laminar layer near the leading edge which change the initial conditions of the turbulent layer a sufficient amount to mask the expected adverse effect.

The large differences in the type of stall and scale effect of the thinner sections as compared with those of the 18-percent-thick airfoil have already been pointed out. The data obtained in previously mentioned unpublished stall studies show gradual separation of the turbulent boundary layer near the trailing edge to limit the lift of the 18-percent-thick section. The character of the lift-curve peak of the NACA 63_3–018 airfoil (fig. 6) as compared with that of the thinner sections also gives some indication that turbulent separation is limiting the lift of the 18-percent-thick section. In view of the preceding discussion of the effect of Reynolds number on turbulent separation, however, the only explanation for the large scale effect shown by this airfoil would seem to be associated with rapidly changing initial conditions of the turbulent layer near the leading edge as the Reynolds number is varied. For an explanation of the variation of these initial conditions, the behavior of the short laminar layer near the leading edge must again be examined.

The pressure gradients near the leading edge of the 18-percent-thick section, although not sufficiently adverse to cause complete separation at the Reynolds numbers of this investigation, might be great enough to produce a laminar-separation bubble of the type previously described. A steady decrease in size of this bubble with increasing Reynolds number could probably cause a favorable change in the initial conditions of the turbulent layer of such magnitude that turbulent separation at the rear would be delayed to higher lift coefficients. Such a phenomenon would account for the variation of the maximum lift with Reynolds number for the 18-percent-thick section. It seems reasonable to suppose, however, that, at some higher value of the Reynolds number, the bubble would be nonexistent and, at an even higher Reynolds number, the laminar layer would be so thin that further decrease in its thickness resulting from increasing Reynolds number would have little effect on the initial conditions of the turbulent layer. When such a condition is reached, the maximum lift would presumably decrease somewhat with further increases in Reynolds number. An indication that this type of scale effect would actually occur may be found in the results for the NACA 8318 airfoil which are discussed in reference 5.

Although the characteristic shape of the curve of maximum lift against Reynolds number is essentially the same for the airfoils of 12 percent thickness and less, the values of the Reynolds number at which the different effects occur vary somewhat with the airfoil thickness and thickness form (figs. 12 (a) and 12 (b)). One effect upon the variation of maximum lift with Reynolds number of increasing the airfoil thickness ratio seems to be a decrease of the value of the Reynolds number at which the maximum lift begins to increase rapidly with Reynolds number (fig. 12 (a)). An increase in airfoil thickness ratio causes the severity of the surface curvature near the leading edge to be reduced which in turn decreases the magnitude of the adverse pressure gradient just behind the leading edge. When considered in relation to the previous qualitative discussion of the mechanism of maximum lift, these two effects of increasing thickness would tend to explain the experimental results. The data of figure 12 (a) also show the magnitude of the favorable scale effect to decrease somewhat with airfoil thickness up to thickness ratios of 12 percent of the chord. A change in the relative strength of the tendency toward laminar separation at the leading edge and turbulent separation at the trailing edge is probably responsible for this behavior.

The data pertaining to the effect of thickness form upon the maximum lift are restricted to movement of the position of minimum pressure on the basic thickness form at zero lift from 30 percent to 50 percent chord and from 30 percent to 40 percent chord for airfoil-thickness ratios of 6 and 9 percent of the chord, respectively. For these thickness ratios, the position of minimum pressure does not appear to have a very powerful effect upon the maximum lift (fig. 12 (b)). Between Reynolds numbers of 15.0×10^6 and 25.0×10^6, the data for the airfoils of 6 percent thickness seem to indicate that moving the position of minimum pressure rearward decreases the maximum lift and delays the rapid rise in maximum lift with Reynolds number. The results, however, are not entirely consistent. Moving the position of minimum pressure rearward has somewhat the same effect upon the surface curvature and the resultant pressure gradients near the leading edge as decreasing the thickness ratio for a given position of minimum pressure. Rearward movement of the position of minimum pressure would, therefore, be expected to shift to higher values the Reynolds number at which the rapid rise in maximum lift with Reynolds number begins. For the very thin airfoils, however, the effect does not appear to be important. On the other hand, the data of reference 1 show that, at Reynolds numbers between 3.0×10^6 and 9.0×10^6, moving the position of minimum pressure rearward has a definitely adverse effect upon the maximum lift of the thicker airfoils.

The effect upon the maximum lift of the addition of a small amount of the uniform load type of camber to the 63-series airfoils of 9 percent thickness and 12 percent thickness is shown in figure 12 (c). The camber increases the maximum lift of both airfoils at all Reynolds numbers but does not materially change the general character of the scale-effect curves. The value of the Reynolds number at which the maximum lift rises rapidly, however, is lowered when camber is added to the 9-percent-thick section. Since camber so changes the curvature of the airfoil surface near the leading edge that the separated laminar layer may attach itself to the surface more readily, this result is not surprising.

The results obtained for the NACA 63–009 airfoil section equipped with a $0.20c$ simulated split flap deflected 60° are also presented in figure 12 (c). These data show the scale-effect curve for the airfoil with split flap to parallel that for the plain airfoil throughout the range of Reynolds number. This result would seem to indicate that the relationship between the various parameters which have been suggested as controlling the maximum lift is unchanged by the deflection of a split flap. Sufficient data are not available, however, to show the general validity of this result.

The fact should be remembered that the discussion of the effects of camber is based on tests of thin NACA 6-series sections having small amounts of the uniform load type of camber. Accordingly, the conclusion cannot be made that the effect of different types and amounts of camber in combination with different types of basic thickness forms would be the same as that shown by the present tests. Similarly, the results obtained for the 9-percent-thick section with split flap are not necessarily results that might be obtained with other types of flaps on other airfoils.

Tests of the NACA 63–009 airfoil with a roughened leading edge (fig. 12 (a)) show that the maximum lift remains relatively constant throughout the Reynolds number range of the tests. The roughness at the leading edge, of course, causes the boundary-layer flow to be turbulent over the entire airfoil. From a consideration of this fact in relation to the previous discussion of turbulent separation, the absence of scale effect for the rough condition might have been expected.

CONCLUDING REMARKS

Results are presented of an investigation made to determine the two-dimensional lift and drag characteristics of nine NACA 6-series airfoil sections at Reynolds numbers of 15.0×10^6, 20.0×10^6, and 25.0×10^6. Also presented are data from NACA Rep. 824 for the same airfoils at Reynolds numbers of 3.0×10^6, 6.0×10^6, and 9.0×10^6. Qualitative explanations in terms of flow behavior are advanced for the observed types of scale effect.

The discussion of the phenomena at maximum lift is particularly speculative and indicates that much more research is necessary before this problem can be analyzed quantitatively. In particular, quantitative data relating to the mechanism controlling the reattachment of the separated laminar layer to the surface and the conditions of the turbulent layer following reattachment are necessary. Should a general investigation of these problems yield fruitful results, it is believed that, with the aid of the relations for turbulent separation previously developed by the NACA, an intelligent approach to the calculation of the maximum lift coefficient for different airfoils at different Reynolds numbers could be made.

Until such time as calculations of this nature are possible, the most important conclusion to be drawn from the maximum lift results of this investigation, from a consideration of airplane design, relates to the comparison of the airfoils at different Reynolds numbers. Although the airfoils of 12 percent thickness and less had the same type of scale-effect curves, the Reynolds numbers at which the different effects predominate varied. The 18-percent-thick section had a type of maximum-lift variation with the Reynolds number that was entirely different from the thinner sections. Any comparison of airfoil maximum-lift characteristics can be made only if the data for the group of airfoils under consideration are available at the same Reynolds number. The choice of an optimum airfoil for maximum lift for a given application, therefore, must be determined from data corresponding to the operating Reynolds number of the application.

LANGLEY AERONAUTICAL LABORATORY,
NATIONAL ADVISORY COMMITTEE FOR AERONAUTICS,
LANGLEY AIR FORCE BASE, VA., *October 13, 1948.*

REFERENCES

1. Abbott, Ira H., Von Doenhoff, Albert E., and Stivers, Louis S., Jr.: Summary of Airfoil Data. NACA Rep. 824, 1945.
2. Von Doenhoff, Albert E., and Abbott, Frank T., Jr.: The Langley Two-Dimensional Low-Turbulence Pressure Tunnel. NACA TN 1283, 1947.
3. Schlichting, H., and Ulrich, A.: Zur Berechnung des Umschlages laminar/turbulent. Jahbr. 1942 der deutschen Luftfahrtforschung, R. Oldenbourg (Munich), pp. I 8–I 35.
4. Prandtl, L.: The Mechanics of Viscous Fluids. Turbulent Flow along a Wall with Special Reference to the Frictional Resistance of Plates. Vol. III of Aerodynamic Theory, div. G, sec. 23, W. F. Durand, ed., Julius Springer (Berlin), 1935, pp. 145–154.
5. Jacobs, Eastman N., and Sherman, Albert: Airfoil Section Characteristics as Affected by Variations of the Reynolds Number. NACA Rep. 586, 1937.
6. Von Doenhoff, Albert E.: A Preliminary Investigation of Boundary-Layer Transition along a Flat Plate with Adverse Pressure Gradient. NACA TN 639, 1938.
7. Von Doenhoff, Albert E., and Tetervin, Neal: Investigation of the Variation of Lift Coefficient with Reynolds Number at a Moderate Angle of Attack on a Low-Drag Airfoil. NACA CB, Nov. 1942.
8. Pinkerton, Robert M.: Calculated and Measured Pressure Distributions over the Midspan Section of the N.A.C.A. 4412 Airfoil. NACA Rep. 563, 1936.
9. Von Doenhoff, Albert E., and Tetervin, Neal: Determination of General Relations for the Behavior of Turbulent Boundary Layers. NACA Rep. 772, 1943.

TABLE I.—ORDINATES OF AIRFOIL SECTIONS

NACA 63–006

[Stations and ordinates given in percent of airfoil chord]

Upper surface		Lower surface	
Station	Ordinate	Station	Ordinate
0	0	0	0
.5	.503	.5	−.503
.75	.609	.75	−.609
1.25	.771	1.25	−.771
2.5	1.057	2.5	−1.057
5	1.462	5	−1.462
7.5	1.766	7.5	−1.766
10	2.010	10	−2.010
15	2.386	15	−2.386
20	2.656	20	−2.656
25	2.841	25	−2.841
30	2.954	30	−2.954
35	3.000	35	−3.000
40	2.971	40	−2.971
45	2.877	45	−2.877
50	2.723	50	−2.723
55	2.517	55	−2.517
60	2.267	60	−2.267
65	1.982	65	−1.982
70	1.670	70	−1.670
75	1.342	75	−1.342
80	1.008	80	−1.008
85	.683	85	−.683
90	.383	90	−.383
95	.138	95	−.138
100	0	100	0

L.E. radius: 0.297

NACA 63–009

[Stations and ordinates given in percent of airfoil chord]

Upper surface		Lower surface	
Station	Ordinate	Station	Ordinate
0	0	0	0
.5	.749	.5	−.749
.75	.906	.75	−.906
1.25	1.151	1.25	−1.151
2.5	1.582	2.5	−1.582
5	2.196	5	−2.196
7.5	2.655	7.5	−2.655
10	3.024	10	−3.024
15	3.591	15	−3.591
20	3.997	20	−3.997
25	4.275	25	−4.275
30	4.442	30	−4.442
35	4.500	35	−4.500
40	4.447	40	−4.447
45	4.296	45	−4.296
50	4.056	50	−4.056
55	3.739	55	−3.739
60	3.358	60	−3.358
65	2.928	65	−2.928
70	2.458	70	−2.458
75	1.966	75	−1.966
80	1.471	80	−1.471
85	.990	85	−.990
90	.550	90	−.550
95	.196	95	−.196
100	0	100	0

L.E. radius: 0.631

NACA 63_1–012

[Stations and ordinates given in percent of airfoil chord]

Upper surface		Lower surface	
Station	Ordinate	Station	Ordinate
0	0	0	0
.5	.985	.5	−.985
.75	1.194	.75	−1.194
1.25	1.519	1.25	−1.519
2.5	2.102	2.5	−2.102
5	2.925	5	−2.925
7.5	3.542	7.5	−3.542
10	4.039	10	−4.039
15	4.799	15	−4.799
20	5.342	20	−5.342
25	5.712	25	−5.712
30	5.930	30	−5.930
35	6.000	35	−6.000
40	5.920	40	−5.920
45	5.704	45	−5.704
50	5.370	50	−5.370
55	4.935	55	−4.935
60	4.420	60	−4.420
65	3.840	65	−3.840
70	3.210	70	−3.210
75	2.556	75	−2.556
80	1.902	80	−1.902
85	1.274	85	−1.274
90	.707	90	−.707
95	.250	95	−.250
100	0	100	0

L.E. radius: 1.087

NACA 63_2–018

[Stations and ordinates given in percent of airfoil chord]

Upper surface		Lower surface	
Station	Ordinate	Station	Ordinate
0	0	0	0
.5	1.404	.5	−1.404
.75	1.713	.75	−1.713
1.25	2.217	1.25	−2.217
2.5	3.104	2.5	−3.104
5	4.362	5	−4.362
7.5	5.308	7.5	−5.308
10	6.068	10	−6.068
15	7.225	15	−7.225
20	8.048	20	−8.048
25	8.600	25	−8.600
30	8.913	30	−8.913
35	9.000	35	−9.000
40	8.845	40	−8.845
45	8.482	45	−8.482
50	7.942	50	−7.942
55	7.256	55	−7.256
60	6.455	60	−6.455
65	5.567	65	−5.567
70	4.622	70	−4.622
75	3.650	75	−3.650
80	2.691	80	−2.691
85	1.787	85	−1.787
90	.985	90	−.985
95	.348	95	−.348
100	0	100	0

L.E. radius: 2.120

NACA 63–209

[Stations and ordinates given in percent of airfoil chord]

Upper surface		Lower surface	
Station	Ordinate	Station	Ordinate
0	0	0	0
.437	.796	.563	−.696
.680	.973	.320	−.833
1.170	1.255	1.330	−1.041
2.408	1.765	2.592	−1.393
4.897	2.510	5.103	−1.878
7.394	3.077	7.606	−2.229
9.894	3.539	10.106	−2.505
14.901	4.263	15.099	−2.917
19.912	4.792	20.088	−3.200
24.925	5.169	25.075	−3.379
29.940	5.414	30.060	−3.470
34.956	5.530	35.044	−3.470
39.971	5.518	40.029	−3.376
44.986	5.391	45.014	−3.201
50.000	5.159	50.000	−2.953
55.012	4.834	54.988	−2.644
60.022	4.429	59.978	−2.287
65.029	3.958	64.971	−1.898
70.033	3.430	69.967	−1.486
75.034	2.861	74.966	−1.071
80.032	2.267	79.968	−.675
85.027	1.663	84.973	−.317
90.019	1.067	89.981	−.033
95.009	.512	94.991	.120
100.000	0	100.000	0

L.E. radius: 0.631
Slope of radius through L.E.: 0.0842

NACA 63_1–212

[Stations and ordinates given in percent of airfoil chord]

Upper surface		Lower surface	
Station	Ordinate	Station	Ordinate
0	0	0	0
.417	1.032	.583	−.932
.657	1.260	.343	−1.120
1.145	1.622	1.355	−1.408
2.378	2.284	2.622	−1.912
4.863	3.238	5.137	−2.606
7.358	3.963	7.642	−3.115
9.859	4.554	10.141	−3.520
14.868	5.470	15.132	−4.124
19.882	6.137	20.118	−4.545
24.900	6.606	25.100	−4.816
29.920	6.901	30.080	−4.957
34.941	7.030	35.059	−4.970
39.962	6.991	40.038	−4.849
44.982	6.799	45.018	−4.609
50.000	6.473	50.000	−4.267
55.016	6.030	54.984	−3.840
60.029	5.491	59.971	−3.349
65.038	4.870	64.962	−2.810
70.043	4.182	69.957	−2.238
75.045	3.451	74.955	−1.661
80.042	2.698	79.958	−1.106
85.035	1.947	84.965	−.601
90.025	1.224	89.975	−.190
95.012	.556	94.988	.066
100.000	0	100.000	0

L.E. radius: 1.067
Slope of radius through L.E.: 0.0842

NACA 64–006

[Stations and ordinates given in percent of airfoil chord]

Upper surface		Lower surface	
Station	Ordinate	Station	Ordinate
0	0	0	0
.5	.494	.5	−.494
.75	.596	.75	−.596
1.25	.754	1.25	−.754
2.5	1.024	2.5	−1.024
5	1.405	5	−1.405
7.5	1.692	7.5	−1.692
10	1.928	10	−1.928
15	2.298	15	−2.298
20	2.572	20	−2.572
25	2.772	25	−2.772
30	2.907	30	−2.907
35	2.981	35	−2.981
40	2.995	40	−2.995
45	2.919	45	−2.919
50	2.775	50	−2.775
55	2.575	55	−2.575
60	2.331	60	−2.331
65	2.050	65	−2.050
70	1.740	70	−1.740
75	1.412	75	−1.412
80	1.072	80	−1.072
85	.737	85	−.737
90	.423	90	−.423
95	.157	95	−.157
100	0	100	0

L.E. radius: 0.256

NACA 64–009

[Stations and ordinates given in percent of airfoil chord]

Upper surface		Lower surface	
Station	Ordinate	Station	Ordinate
0	0	0	0
.5	.739	.5	−.739
.75	.892	.75	−.892
1.25	1.128	1.25	−1.128
2.5	1.533	2.5	−1.533
5	2.109	5	−2.109
7.5	2.543	7.5	−2.543
10	2.898	10	−2.898
15	3.455	15	−3.455
20	3.868	20	−3.868
25	4.170	25	−4.170
30	4.373	30	−4.373
35	4.479	35	−4.479
40	4.490	40	−4.490
45	4.364	45	−4.364
50	4.136	50	−4.136
55	3.826	55	−3.826
60	3.452	60	−3.452
65	3.026	65	−3.026
70	2.561	70	−2.561
75	2.069	75	−2.069
80	1.564	80	−1.564
85	1.069	85	−1.069
90	.611	90	−.611
95	.227	95	−.227
100	0	100	0

L.E. radius: 0.579

NACA 65–006

[Stations and ordinates given in percent of airfoil chord]

Upper surface		Lower surface	
Station	Ordinate	Station	Ordinate
0	0	0	0
.5	.476	.5	−.476
.75	.574	.75	−.574
1.25	.717	1.25	−.717
2.5	.956	2.5	−.956
5	1.310	5	−1.310
7.5	1.589	7.5	−1.589
10	1.824	10	−1.824
15	2.197	15	−2.197
20	2.482	20	−2.482
25	2.697	25	−2.697
30	2.852	30	−2.852
35	2.952	35	−2.952
40	2.998	40	−2.998
45	2.983	45	−2.983
50	2.900	50	−2.900
55	2.741	55	−2.741
60	2.518	60	−2.518
65	2.246	65	−2.246
70	1.935	70	−1.935
75	1.594	75	−1.594
80	1.233	80	−1.233
85	.865	85	−.865
90	.510	90	−.510
95	.195	95	−.195
100	0	100	0

L.E. radius: 0.240